Variance Risk Premium Components and International Stock Return Predictability*

Juan M. Londono† Federal Reserve Board

Nancy R. Xu‡ Boston College

March 19, 2020

Abstract

We decompose the U.S. variance risk premium (VP) into its downside and upside components (DVP and UVP, respectively) as proxies for asymmetric global risk variables, and find that acknowledging for asymmetry in VP significantly improves its international stock return predictability. To rationalize our empirical findings, we propose an international dynamic asset pricing model featuring asymmetric non-Gaussian shocks and partial global integration. We find that (i) DVP (UVP) is mostly driven by global risk aversion (economic uncertainty), (ii) international equity risk premiums exhibit distinct loadings on global premium determinants, and (iii) DVP (UVP) transmits to international markets through financial (economic) integration.

JEL Classification: F36, G12, G13, G15.
Keywords: Downside variance risk premium, Upside variance risk premium, International stock markets, Asymmetric state variables, Stock return predictability.

*The views expressed in this document do not necessarily reflect those of the Federal Reserve System or its staff. We would like to thank Kasper Joergensen (discussant), Terry Pan (discussant), Dacheng Xiu, Hao Zhou, and seminar/conference participants at Boston College (Carroll), Boston Macro Juniors Workshop (MIT Sloan), 2018 Econometric Society European winter meeting, 2018 China International Risk Forum, 2019 Midwest Finance Association annual meeting, 2019 Eastern Finance Association annual meeting, 2019 FMA Global Conference in Latin America, 2019 ECWFC at WFA, 2019 NASMES Summer Meeting, and 2019 Stanford SITE "Session 7: Asset Pricing Theory". First circulated version: November 17, 2018. An Internet Appendix is available at `https://www.nancyxu.net/research`. All errors are our own.

†Division of International Finance, Federal Reserve Board U.S., 20th Street and Constitution Avenue N.W., Washington, DC 20551; email: juan.m.londono@frb.gov.

‡Boston College, Carroll School of Management, 140 Commonwealth Avenue, Chestnut Hill, MA, 02467, U.S.; email: nancy.xu@bc.edu.

Variance Risk Premium Components and International Stock Return Predictability

Abstract

We decompose the U.S. variance risk premium (VP) into its downside and upside components (DVP and UVP, respectively) as proxies for asymmetric global risk variables, and find that acknowledging for asymmetry in VP significantly improves its international stock return predictability. To rationalize our empirical findings, we propose an international dynamic asset pricing model featuring asymmetric non-Gaussian shocks and partial global integration. We find that (i) DVP (UVP) is mostly driven by global risk aversion (economic uncertainty), (ii) international equity risk premiums exhibit distinct loadings on global premium determinants, and (iii) DVP (UVP) transmits to international markets through financial (economic) integration.

JEL Classification: F36, G12, G13, G15.
Keywords: Downside variance risk premium, Upside variance risk premium, International stock markets, Asymmetric state variables, Stock return predictability.

1. Introduction

Since the global financial crisis, there has been renewed interest in understanding how asset returns comove across countries. While the recent literature aims to document and rationalize various sources of global risk (see, e.g., Miranda-Agrippino and Rey (2018) and Xu (2019)), we center the attention on *asymmetric* global risk variables and highlight their distinct asset pricing implications. In particular, we study the U.S. variance risk premium (henceforth VP) as a proxy for global risk and decompose it into its downside (DVP) and upside (UVP) components that, respectively, capture compensations for bearing variance risk emanating from the left and right tails of the stock return distribution. We establish new stylized facts on the dynamics of DVP and UVP and document their distinct international stock return predictability patterns. Then, we rationalize these findings with an international no-arbitrage dynamic asset pricing model featuring asymmetric risk premium state variables and international spillovers. Together with our empirical findings, our model aims to identify economic sources and international transmission channels of DVP and UVP.

To obtain the asymmetric components of VP, we explore a wide range of alternative measures. DVP and UVP are estimated as the difference between the risk-neutral and physical expectations of one-month-ahead stock return variance, conditional on whether the one-month-ahead stock price is below (bad states) or above (good states) the current stock price, respectively. In particular, we approximate the risk-neutral expectation of the downside (upside) stock return variance using puts (calls) on the S&P 500 index at different strikes and maturities; and we obtain the physical expectation of the downside (upside) stock return variation using the best forecast of the downside (upside) realized variance. Our sample spans from April 1991 to March 2018.

We document stylized facts of VP, DVP, and UVP from four aspects: magnitude, cyclicality, relativity, and persistence. We find that the total VP and its downside component are highly correlated, on average positive, and significant. Both VP and DVP are countercyclical, with large positive spikes around key episodes of market stress and economic turmoil. In contrast, UVP, although positive, on average, is borderline significant and displays occasional negative spikes. UVP exhibits a much more transitory and procyclical behavior with large negative spikes that coincide with some of the large positive DVP spikes. These different dynamics suggest that, during normal periods, investors dislike downside variance risk and mostly

disregard upside variance risk. However, during episodes of economic turmoil, investors appear to dislike downside variance risk even more, but prefer to be paid to hold a hedging position against possible future large returns. Overall, the distinct dynamics of DVP and UVP indicate that investors distinguish the pricing of downside and upside stock return variance risks.

In our main empirical finding, we show that acknowledging for asymmetry in VP significantly improves its international stock return predictability, and that both DVP and UVP are useful predictors of international stock returns with distinct predictability patterns. We consider U.S. dollar excess returns of 22 countries' representative stock indexes, as commonly applied in the international comovement literature (e.g., Bekaert, Hodrick, and Zhang (2009); Christoffersen, Errunza, Jacobs, and Langlois (2012); Xu (2019); among many others). The international stock return predictability improves the most at horizons of less than six months. The predictive power of DVP, like that of the total VP, follows a hump-shaped pattern peaking at mid horizons, between four and six months, while that of UVP follows a decreasing pattern peaking at very short horizons. The predictability patterns are robust to considering country-level or panel regression specifications, using alternative estimates of the VP components, and adding other control predictors such as the U.S. dividend yield and term spread. The international return predictability results of DVP and UVP are, to the best of our knowledge, new to the literature.

In the second part of the paper, we solve an international no-arbitrage dynamic asset pricing model to rationalize the different dynamic behaviors and international stock return predictability patterns of DVP and UVP. This international model has two key features. On the one hand, because this paper focuses on the asymmetry of risk premiums, the model allows for flexible shock assumptions to introduce asymmetries into the dynamics of both economic fundamentals and investors' attitudes toward risk. On the other hand, we allow for a partially-integrated world economy, wherein each country's representative agent has a habit-type utility function that is a nonlinear combination of a global part and an idiosyncratic part. Given the moment generating function of the shock structure and the no-arbitrage condition, the model is in the exponential affine class. The model solution suggests economic determinants of VP and its components and international equity risk premiums, hence shedding light on stock return predictability.

After bringing the model solution to empirical estimates of the VP components, we find that the upside movements in risk aversion, a price-of-risk state variable, accounts for the largest

fraction (41%) of the total variation in DVP. Through the lens of our model, one standard deviation (SD) increase in risk aversion increases DVP by 8.5∼10 (monthly percentage squared), with a slightly more positive relation in worse economic conditions. In contrast, UVP is significantly more sensitive to economic uncertainty, an amount-of-risk state variable. The relation between UVP and economic uncertainty is highly nonlinear: on average, one SD increase in the downside economic uncertainty dampens UVP by around 2 (monthly percentage squared), but when the current economic condition declines to its lower 1st percentile (e.g. during the Lehman Brothers aftermath), one SD increase in downside economic uncertainty dampens UVP by 29 — a drop that is almost 8 times the sample standard deviation of UVP. Hence, our findings suggest that, when risk aversion increases persistently, investors are willing to pay more to hedge against future downside variance risk, resulting in a countercyclical and relatively persistent DVP (as established earlier). On the other hand, the pricing of upside variance risk appears to be more sensitive to both expected and realized economic conditions, potentially explaining the procyclical and relatively more transitory nature of UVP.

Then, we provide insights on the distinct international predictability patterns of DVP and UVP by matching the empirical predictive coefficient estimates (from the first part of the paper). We find that the hump-shaped predictability pattern of DVP can be explained by the fact that international equity risk premiums increase with global risk aversion, with loading coefficients peaking at the four- to six-month horizons. The decreasing predictability pattern of UVP can be explained by equity risk premium loadings on the global downside economic uncertainty that are negative at very short horizons but become positive at horizons longer than seven months. This way, we uncover the latent relation between economic uncertainty and equity risk premiums by incorporating information from international predictability patterns of VP components.

Finally, our framework identifies the transmission/integration channels of global risk variables to international stock markets by exploiting both the cross-horizon and cross-country predictive coefficients. We find that international transmission channels are in line with the different economic interpretations of DVP and UVP. In particular, financial integration, proxied by each country's credit-to-GDP ratio, is more important in transmitting the pricing information carried by DVP, while real economic integration, proxied by each country's trade-to-GDP ratio, is a more important transmission channel of UVP.

1.1. Related literature and contributions

Our paper is related to the growing literature documenting the variance risk premium and its predictive power for asset returns. Bollerslev, Tauchen, and Zhou (2009) and Drechsler and Yaron (2010), among others, find empirical evidence that the U.S. VP is a useful predictor of U.S. stock returns. Several papers have documented the predictive power of U.S. VP for other U.S. assets' returns (see, for instance, Zhou (2010)). In an international setting, Londono and Zhou (2017) find evidence that U.S. VP also has predictive power for the appreciation rate of several currencies against the U.S. dollar; Londono (2015) and Bollerslev, Marrone, Xu, and Zhou (2014) explore the predictability of local and U.S. VP on international stock returns. In this paper, we take the perspective of a global/U.S. investor in both the empirical and theoretical parts. We contribute to this literature by showing that decomposing VP into its downside and upside components yields higher predictability for international stock returns than using the total VP.

In addition, the recent literature has highlighted potentially different compensations for bearing stock return variations associated with good and bad states. The measurement of these compensations (DVP and UVP) is still an ongoing debate (see, e.g., Kilic and Shaliastovich (2018), Held, Kapraun, Omachel, and Thimme (2018), and Feunou, Jahan-Parvar, and Okou (2017)). In particular, a popular measure uses past realized semivariances as the expected future realized semivariances (Kilic and Shaliastovich (2018)). We contribute to this literature by examining a wide range of models to obtain the physical expectation of downside and upside realized semivariances and, thus, to calculate the VP components. We show improvements in separating the dynamic behaviors of DVP and UVP.

Adding to our empirical contributions, we also discuss the potential economic interpretation of VP. Bollerslev, Tauchen, and Zhou (2009) interpret VP in a general equilibrium model with recursive preferences and time-varying variance of variance of consumption growth (see an international version in Londono (2015)); Bekaert, Engstrom, and Xu (2020) document a potentially close relation between the model-implied VP and investors' relative risk aversion while imposing pricing consistency within two major risky asset markets (equities and corporate bonds). Our reduced-form asset pricing framework acknowledges both volatility of volatility of fundamental growth rates and risk aversion as important premium determinants in explaining VP and its components. By bringing the model solution to empirical estimates of DVP and

UVP, we are among the first to propose, with plausible quantitative measures, that different premium determinants weight differently in explaining their distinct dynamic behaviors.

One of the advantages of studying international stock return predictability is to incorporate more information to understand the risk transmission mechanism of these asymmetric global variables. Our theoretical framework and the international predictive coefficient estimates allow us to test the relative importance of financial and economic integration in explaining the international pricing of global risk variables. The main premium determinant of DVP – risk aversion – transmits through financial integration channels to international stock markets, which formally supports Gourinchas and Jeanne (2006), Colacito and Croce (2010), and Stiglitz (2010) using a completely different framework. We also document that the main premium determinant of UVP – economic uncertainty – transmits through trade/real economic integration; to the best of our knowledge, our paper is among the first to document the importance of trade integration in the transmission of economic uncertainty. Our contribution is to document both channels through one unified parsimonious asset pricing framework.

The remainder of the paper is organized as follows. Section 2 constructs upside and downside VP components and compares their behaviors. Section 3 documents the distinct international stock return predictability patterns of DVP and UVP. Section 4 solves an international dynamic asset pricing model to rationalize our main empirical findings. Concluding remarks are included in Section 5.

2. VP and Its Downside and Upside Components

In this section, we measure and explore the time series behaviors of the downside and upside components of the variance risk premium.

2.1. Definitions

We follow the notation in Bollerslev, Tauchen, and Zhou (2009) and define the total one-month-ahead VP as the difference between the risk-neutral (Q) and the physical (P) expectations of the total variance of one-month-ahead stock returns,

$$VP_{t,t+1} = V_t^Q(r_{t+1}) - V_t^P(r_{t+1}), \tag{1}$$

where r_{t+1} denotes the log stock return between months t and $t+1$. We decompose VP into its downside and upside components, which we label DVP and UVP, respectively. These

components allow us to disentangle the compensations for bearing downside and upside variance risks. We estimate the risk-neutral and physical components of DVP and UVP separately.

The risk-neutral components are extracted from option prices using what is usually known as the model-free methodology (see Britten-Jones and Neuberger (2000)). Specifically, following Andersen and Bondarenko (2009), we approximate the risk-neutral components of DVP and UVP using the option-implied downside and upside variances, respectively, as follows:

$$iv^{D}_{t,t+1} = \left(\int_{0}^{S_t} \frac{2(1 + log(S_t/K)}{K^2} P(t+1,K) dK \right)^2, \tag{2}$$

$$iv^{U}_{t,t+1} = \left(\int_{S_t}^{\infty} \frac{2(1 - log(K/S_t)}{K^2} C(t+1,K) dK \right)^2,$$

where S_t is the current stock index price and $P(K)$ ($C(K)$) is the price of a put (call) with strike K and a one-month maturity. Intuitively, the option-implied downside (upside) variance is identified by put (call) options that pay off when the return realization is negative (positive).

We approximate the physical components of DVP and UVP using the expected values of one-month-ahead downside and upside realized variances, respectively. Following the convention in the literature (see Feunou, Jahan-Parvar, and Okou (2017); Kilic and Shaliastovich (2018); Held, Kapraun, Omachel, and Thimme (2018); and Baele, Driessen, Ebert, Londono, and Spalt (2018)), the realized semivariances are obtained as follows:

$$rv^{D}_{t+1} = \sum_{\tau=1}^{N} r_{\tau}^2 1_{r_\tau < 0}, \tag{3}$$

$$rv^{U}_{t+1} = \sum_{\tau=1}^{N} r_{\tau}^2 1_{r_\tau > 0},$$

where r_τ represents the instantaneous return calculated using stock prices sampled at high frequencies (every 5 or 15 minutes) between months t and $t+1$ and N is the total number of high-frequency return observations within the month. Intuitively, we separate the return variability due to negative and positive price movements. The physical expectations of downside and upside realized variances are obtained using simple projections:

$$E_t(rv^{i}_{t+1}) = \hat{\alpha}^{i} + \hat{\boldsymbol{\gamma}}^{\boldsymbol{i}} \boldsymbol{X}^{\boldsymbol{i}}_{\boldsymbol{t}}, \tag{4}$$

where $i = D$ or U for downside and upside, respectively, and $\mathbf{X^i_t}$ is a chosen set of predictors observable at time t. We allow $\mathbf{X^i_t}$ to be different in predicting downside and upside realized variances, capturing the possibly different economic determinants of left and right return tails.

Therefore, DVP and UVP are obtained, respectively, as follows:

$$vp^D_{t,t+1} = iv^D_{t,t+1} - E_t(rv^D_{t+1}), \tag{5}$$

$$vp^U_{t,t+1} = iv^U_{t,t+1} - E_t(rv^U_{t+1}).$$

2.2. Measures

We use daily prices for options on the S&P 500 index at different strikes and maturities (source: OptionMetrics) to obtain the risk-neutral components of DVP and UVP. We then use intradaily prices sampled every 15 minutes for this stock index (source: TICKDATA) to obtain the realized semivariances. Our sample period is between April 1991 and March 2018.

Figure 1 shows the time variation in the option-implied variance (top) and its downside and upside components (bottom). The dynamics of option-implied variances confirm the statistics reported in Kilic and Shaliastovich (2018). In addition, the downside implied variance accounts for a larger fraction of the total implied variance than its upside component during almost all times; the fraction is around 60% (75%) before (after) the 2007-08 global financial crisis, but rises to as high as 97% during the peak. The total implied variance is highly correlated with its components (0.99 with DVP and 0.96 with UVP). All three time series spike around crisis periods in our sample, including the Long-Term Capital Management fund crisis in the late 1990s, the corporate scandals in the early 2000s, the collapse of Lehman Brothers during the global financial crisis, and the European debt crisis in the late 2011.

Next, we measure the physical expectations of return semivariances. While the literature has proposed and compared various models for predicting the total realized variance (see, e.g., Bekaert and Hoerova (2014) for a thorough discussion), there is limited research on predicting the downside and upside realized variances. Table 1 explores seven forecast specifications of one-month-ahead realized semivariances at the daily frequency using the regression framework in Equation (4). The specification in measure (1) assumes that realized semivariances follow a Martingale process, as in Bollerslev, Tauchen, and Zhou (2009) and Kilic and Shaliastovich (2018); that is,

$$E_t(rv^i_{t+1}) = rv^i_t. \tag{6}$$

From columns (2) to (7), we consider various combinations of predictors including past realized variance and semivariances calculated at various frequencies. Simple AR(1) forecasts of downside and upside realized variances (measure (2)) yield considerable improvements in terms of

adjusted R^2s and BICs with respect to the Martingale specification (measure (1)). Including the total variance to the simple AR(1) specification, as seen in column (3), lowers the BIC but the high correlation among the two predictors makes the regression difficult to interpret. On the other hand, according to column (4), a heterogeneous autoregressive (HAR) framework using the past monthly ($rv^i_{t-1m,t}$), weekly ($rv^i_{t-5d,t}$), and daily ($rv^i_{t-1d,t}$) realized semivariances also significantly improves the goodness of fit, for both downside and upside realized variances.[1] In particular, realized semivariances calculated over the last week or day of the month are significant and positive predictors, and their predictability is additional to that of the realized semivariance calculated over the entire past month. In columns (5)–(7), we include past total, downside, or upside option-implied variances and evaluate the predictive performances.

Given the model selection criterion, we choose measure (7) as the estimate of the downside physical variance and measure (6) as the estimate of the upside physical variance. Our evidence suggests that the set of informative predictors of downside and upside realized variances can be different, which is new to the literature. Some predictor coefficient estimates in both specifications become insignificant, which is, in part, because of the moderate to high correlations among the predictors. This potential multi-collinearity issue is admitted by several papers in this literature, including Bekaert and Hoerova (2014), however, it is typically left untreated because the goal is forecast improvement rather than coefficient precision.[2]

In sum, with the chosen risk-neutral and physical expected variance estimates, DVP and UVP are obtained given Equation (5). The sum of the two VP components yields the total VP. In the remainder of the paper, we use the end-of-month estimates as our main DVP and UVP measures.

2.3. Time series behaviors

We compare the time series behaviors of monthly DVP and UVP from four perspectives: magnitude, relevance, cyclicality, and persistence. First, from Table 2, the option-implied

[1] This HAR framework for realized semivariances extends Corsi (2009), who focuses on forecasting the total realized variance. Feunou, Jahan-Parvar, and Okou (2017) also consider the HAR framework to approximate the expectations of downside and upside realized variances. However, they do not report the coefficients associated with the HAR components or the fit of the model, and they conclude that the results for the HAR specification are qualitatively similar to those for the Martingale specification.

[2] We are able to replicate and confirm the main result in Bekaert and Hoerova (2014) using our daily data: option-implied variance contains information about future total realized variance, and, therefore, the best forecast specification uses both past realized variances (as in the original Corsi model) and implied variance as predictors. However, neither Corsi (2009) nor Bekaert and Hoerova (2014) forecast downside and upside realized variances as we do here. Additional evidence on our total realized variance forecast results is shown in Table i of the Internet Appendix.

downside variance is on average higher than the expected downside realized variance, yielding a positive DVP with an average of 13.48 squared percent in our chosen model. The positive nature of DVP holds for all other measures in our paper and is consistent with the extant literature (Kilic and Shaliastovich (2018), Feunou, Jahan-Parvar, and Okou (2017), and Held, Kapraun, Omachel, and Thimme (2018)). Our DVP measure is prone to large positive spikes, suggesting a high chance of observing excessive put prices relative to the physical expectation of future stock return variability. For instance, our DVP measure reaches a value of 101.10 squared percent during the peak of 2007-08 financial crisis as shown in Figure 2. However, the DVP measure in Kilic and Shaliastovich (2018) exhibits major negative spikes (i.e., higher physical expectation) during this crisis period, which is likely due to the Martingale assumption when obtaining the physical expectation.[3]

The option-implied upside variance is found to be, on average, higher than the expected upside realized variance; however, UVP is much smaller (0.58) than DVP (13.48), according to Table 2. The average UVP is also significant and positive at the 5% significance level. This finding is potentially different from Kilic and Shaliastovich (2018) and Feunou, Jahan-Parvar, and Okou (2017), who find that UVP is on average negative. In contrast to DVP, our UVP measure is more prone to large negative spikes, as shown in Figure 2. For instance, UVP reached -40.84 squared percent during the Lehman Brothers aftermath, which is almost 13 standard deviations away from its historical average.

Second, we find that the total VP comoves closer to DVP than to UVP. Panel A of Table 3 shows that the correlation between VP and DVP using our chosen models is 0.95, while that between UVP and VP is 0.35. Our DVP and UVP measures are statistically uncorrelated.[4]

Third, DVP is positively correlated with the monthly NBER recession indicator (correlation = 0.42, p-value = 0.00) and negatively correlated with monthly U.S. industrial production growth (correlation = -0.12, p-value = 0.03), rendering a countercyclical DVP; in contrast, UVP

[3]Kilic and Shaliastovich (2018) define VP as the difference between the physical and risk-neutral expectations of the variance, whereas we define VP as risk-neutral minus physical expectation. Realized variance is likely to be extreme and high during economic turmoil, which indicates an extremely high expectation of future market variability given the Martingale assumption and can drive down DVP to a large negative measure (or a large positive measure as in their Figure 3). However, the statistical evidence in our Table 1 shows that the Martingale measure (i.e., measure (1)) has the least predictive power for realized semivariances, when compared to the other models considered. We show the time series of measure (1) using our data in Figure i of the Internet Appendix, and we are able to replicate the main summary statistics in Kilic and Shaliastovich (2018) for this measure.

[4]Panels B and C of Table 3 show correlations across alternative DVP and UVP measures, respectively. The key message is that both the DVP and UVP measures are highly correlated across measures, with a correlation coefficient ranging from 0.74 to 0.99 for DVP and from 0.74 to 0.99 for UVP. Measure (1), or the Martingale measure, exhibits significantly lower correlations with other measures.

is insignificantly correlated with the monthly NBER indicator but weakly and positively correlated with the growth rate (correlation = 0.10, p-value = 0.07), suggesting weakly procyclical dynamics. From Figure 2, DVP displays large and positive spikes around crises, which is also typically observed in total VP (see, e.g., Bollerslev, Gibson, and Zhou (2011), Corradi, Distaso, and Mele (2013), and Bekaert and Hoerova (2014)), while UVP exhibits large negative spikes that tend to coincide with some major positive DVP spikes: for instance, around the Asian crisis in 1997, after the collapse of Lehman Brothers, and during the Greek bailout. Thus, our evidence rejects constant hedging demands and suggests a dynamic relation between the current economic conditions and the compensation demanded for bearing downside and upside variance risks. Under extreme economic and financial conditions, investors seem to separate the pricing of downside and upside variance risks, resulting in the decoupling of DVP and UVP.

Finally, UVP appears to be more transitory than DVP. At the monthly frequency, the AR(1) coefficient of our DVP measure is 0.78, whereas that of our UVP measure is only 0.22. These four empirical facts are robust across alternative measures. Hence, our findings suggest that investors, in general, demand much higher compensations for downside shock exposures than for upside shock exposures, although both shocks lead to increases in total variance. The fact that the historical averages of both VP components are positive indicates that, on average, investors dislike risks emanating from both tails. However, during certain periods (likely to be bad economic environments), we find that compensations demanded for bearing downside and upside variance risks diverge. A more positive DVP indicates a higher demanded compensation, while a lower or even negative UVP suggests that investors demand a negative compensation for bearing upside variance risk. In other words, during these episodes, investors would like to be paid to have a fully-hedged position against the chance of an extreme positive event in the near future.

3. International Stock Return Predictability

In this section, we examine the international stock return predictability patterns of DVP and UVP, our proxies for asymmetric global risk variables. We take the perspective of a global investor whose asset values are denominated in U.S. dollars. Therefore, we consider U.S. dollar excess returns of 22 countries' headline stock market indexes covering North America, Asia, and Europe. Log market returns are obtained from total return indices (source: DataStream),

and the risk free rate uses the zero-coupon yield of U.S. Treasury bonds (source: FRED). As in section 2, the sample period runs from April 1991 to March 2018 (T = 324 months). In Section 3.1, we provide the main predictability results for the country-level and panel predictive regressions. In Section 3.2, we assess the robustness of our results to alternative VP measures (in particular, the Martingale measure) and to control predictors.

3.1. Main predictability results

The main country-level predictability regression, or specification (1), is as follows:

$$h^{-1}r_{i,t,t+h} = a_{i,h} + b_{i,h,D}vp^{D}_{t,t+1} + b_{i,h,U}vp^{U}_{t,t+1} + \epsilon_{i,t+h}, \tag{7}$$

where t denotes the month; $r_{i,t,t+h}$ denotes the h-month-ahead log excess returns for country i; $vp^{D}_{t,t+1}$ and $vp^{U}_{t,t+1}$ denote DVP and UVP, respectively, as constructed in Section 2.

An intuitive null regression specification imposes the same predictive coefficients for DVP and UVP. Table 4 reports the predictive results of the null specification at the country level at 1-, 3-, 6-, and 12-month horizons; the full-horizon predictability patterns are shown in Figure 3. Our results for the U.S. are consistent with those in the domestic return predictability literature (see, e.g., Bollerslev, Tauchen, and Zhou (2009) and Drechsler and Yaron (2010)); in particular, the hump-shaped domestic predictability pattern of the total VP peaks at around the six-month horizon. We also provide evidence that this hump-shaped predictability pattern with significant and positive predictive coefficients holds for almost all countries in our sample, with a few exceptions, such as Belgium, the Netherlands, Ireland, Portugal, and Switzerland.[5]

We then examine whether acknowledging for asymmetry improves the predictability of VP. In Table 5, we compare the bivariate predictive regression (specification (1)) against the null specification in terms of model AIC, BIC, and adjusted R^2.[6] Irrespective of the selection criteria, specification (1), which allows for different DVP and UVP predictive coefficients, significantly outperforms the null specification for all countries and all horizons considered, which is one of the core empirical results of this paper. Figure 4 decomposes the total R^2 of specification (1) into its DVP and UVP contributions for each country. It is clear that the DVP contribution

[5]For Switzerland, the coefficient associated with VP is negative and borderline significant at the one-month horizon. It is noteworthy that our results for this univariate null specification are not immediately comparable to those in Bollerslev, Marrone, Xu, and Zhou (2014) because their country-level evidence (Table 3, pp. 646) uses country-specific VPs and returns denominated in local currencies, whereas our paper takes the perspective of a global investor (i.e., dollar returns and global predictors). Together with their results, our findings suggest that the U.S. VP might also predict changes in exchange rates, which is then consistent with the evidence in Londono and Zhou (2017). However, exploring the effect of VP on exchange rates is not the focus of the present research.

[6]Figure ii in the internet appendix compares the adjusted R^2s of specification (1) with those of the null regression specification for all horizons.

(shaded region) tends to become dominant as the horizon increases, while the UVP contribution is mostly at the very short-horizon. Our results suggest that decomposing VP into its downside and upside components might introduce more flexibility in capturing mixed underlying dynamics of international equity risk premiums at different horizons.

Figures 5 and 6 depict the predictive coefficient estimates and patterns associated with DVP and UVP in specification (1), respectively. At the country level, the hump-shaped pattern of the predictive coefficients of DVP is similar to that of the total VP in Figure 3. However, as shown in Figure 6, the predictive coefficients of UVP exhibit a consistently positive but decreasing pattern for most countries (except for Japan). The predictability pattern of UVP tends to peak at the one-month horizon, drop monotonically after four months, and become insignificant after seven months. The positive estimates of the coefficients of DVP and UVP imply that when investors increase their demand for compensation for bearing downside or upside variance risks, they also bid down the prices of international risky assets and demand high equity risk premiums at 4–6 month horizons following an increase in DVP and at the very-short horizon following an increase in UVP.

To better summarize the country-level results, we estimate a pooled bivariate predictive regression, or specification (2):

$$h^{-1}r_{i,t,t+h} = a_h + b_{h,D}vp^D_{t,t+1} + b_{h,U}vp^U_{t,t+1} + \epsilon_{i,t+h}. \tag{8}$$

The results for this specification are summarized in Table 6 and are consistent with the country-level evidence. Similarly, the coefficient associated with DVP follows a hump-shaped pattern and has the largest coefficient at the six-month horizon (0.2676***), while the coefficient associated with UVP follows a generally decreasing pattern. Moreover, the variance decomposition result confirms that UVP is a dominant predictor relative to DVP only for horizons of less than six months, which is also consistent with our country-level analysis in specification (1).

3.2. Robustness tests

We assess the robustness of our main results to using alternative VP measures and to adding other control predictors. First, we focus on the Martingale measures (measure (1) in Tables 1–3).[7] The predictability patterns of the alternative DVP and UVP measures are shown in Figures 7 and 8, respectively; the model selection results between the null specification

[7]Figure i in the Internet Appendix compares the time series of the Martingale VP measures with the measures used for the main predictability results.

and specification (1) for the Martingale measures are reported in Tables ii and iii of the Internet Appendix. As before, acknowledging for asymmetry in VP improves international stock return predictability. Moreover, the Martingale measure of DVP (UVP) also exhibits the hump-shaped (decreasing) predictability pattern, and both VP components have positive predictive coefficients.

In addition, to assess whether the predictive power of DVP and UVP is additional to that of some well-established stock return predictors, we examine augmented versions of specifications (1) and (2) in which we control for the term spread and the dividend yield at the country and pooled levels, respectively. Figures 5 and 6 plot the predictive coefficient estimates of DVP and UVP with control predictors (i.e., depicted in solid lines with 90% confidence intervals in dashed lines) against those without control predictors (i.e., depicted in red stars, as discussed in Section 3.1). The predictability patterns of both DVP and UVP remain statistically indifferent. Moreover, the variance decomposition results in Figure 9 demonstrate that the fraction of the adjusted R^2 explained by the VP components (indicated in the shaded area) concentrates at shorter horizons. Table 7 summarizes the results for the pooled multivariate predictive specification and confirms that UVP (DVP) exhibits the leading variance decomposition share at very short (mid) horizons, while the dividend yield is a long-horizon predictor. Similar variance decomposition results can be found using the Martingale measure (measure (1)).[8]

4. Economic Interpretations

In this section, we solve an international no-arbitrage dynamic asset pricing model. To maintain the empirical focus of the paper, we match the model solution to the empirical estimates of the VP components in Section 2 to understand their economic determinants, and we match the predictability patterns documented in Section 3 to understand the transmission of DVP and UVP to international equity risk premiums within a consistent asset pricing framework. The model allows for various sources of asymmetry in a reduced form. First, it features asymmetric shocks when modeling the tail behaviors of global premium state variables (time-varying risk aversion and fundamental/economic uncertainty) in this world economy. Second, country-level state variables can have different integration coefficients across countries and state variables. We introduce the reduced-form model in Sections 4.1 and 4.2 and provide the model

[8]Table iv reports the predictive coefficient estimates and adjusted R^2s for the augmented country-level specification. Figure iii shows the variance decomposition among the four predictors in the augmented specification.

solution in Section 4.3. Section 4.4 presents the empirical strategies and the main estimation results.

4.1. The U.S. investor and state variables

Assume that the representative U.S. (global) investor has a period utility function over consumption C_t and a reference level Q_t in the HARA utility class:

$$U(C_t) = \frac{(C_t/Q_t)^{1-\gamma}}{1-\gamma}, \tag{9}$$

where Q_t drives the time variation in the relative risk aversion (RRA_t),

$$RRA_t = -\frac{C_t U''(C_t)}{U'(C_t)} = \gamma Q_t, \tag{10}$$

and γ is the utility curvature parameter. Intuitively, a higher Q_t delivers less consumption utility, hence implying a higher RRA; Campbell and Cochrane (1999) is a special case with $Q_t = \frac{C_t}{C_t - H_t}$, where H_t is the external habit level. The logarithm of the stochastic discount factor (SDF) can be derived as follows:

$$m_{t+1} = \ln(\beta) + \ln\left[\frac{U'(C_{t+1})}{U'(C_t)}\right] = \ln(\beta) - \gamma \Delta c_{t+1} + \gamma \Delta q_{t+1}, \tag{11}$$

where β is a constant time preference parameter, $\Delta c_{t+1} \equiv \ln[C_{t+1}/C_t]$ is the log change in consumption, and Δq_{t+1} captures the log change in the relative risk aversion.

The log consumption growth is assumed to follow a reduced-form dynamic process with asymmetric and heteroskedastic shocks:

$$\Delta c_{t+1} = c_0 + \rho_{cp} cp_t + \rho_{cn} cn_t + \delta_{cp} \omega_{cp,t+1} - \delta_{cn} \omega_{cn,t+1}, \tag{12}$$

where the conditional mean is sensitive to the expected economic upside and downside uncertainties, cp_t and cn_t, respectively. Following Bekaert and Engstrom (2017), the disturbance of the log consumption growth is decomposed into two independent centered gamma shocks:

$$\omega_{cp,t+1} = \Gamma(cp_t, 1) - cp_t, \ \omega_{cn,t+1} = \Gamma(cn_t, 1) - cn_t, \tag{13}$$

where the real upside (downside) shock, denoted as $\omega_{cp,t+1}$ ($\omega_{cn,t+1}$), governs the right-tail (left-tail) dynamics of the growth distribution with shape parameter cp_t (cn_t) determining the conditional higher moments of the shock. For example, given the moment generating function (MGF) of independent gamma shocks, the conditional variance of Δc_{t+1} is $\delta_{cp}^2 cp_t + \delta_{cn}^2 cn_t$ and the conditional unscaled skewness is $2\delta_{cp}^3 cp_t - 2\delta_{cn}^3 cn_t$. Hence, cp_t (cn_t) can be interpreted as the "good" ("bad") uncertainty state variable because it increases (decreases) with the conditional skewness of the future growth rates. This shock assumption is particularly suitable

for the present research because it builds in asymmetric second moments and distributional assumptions in a parsimonious and tractable way, while allowing the model to stay within an affine framework. The dynamics of the upside and downside real uncertainty state variables follow an AR(1) process:

$$cp_{t+1} = cp_0 + \rho_{cpcp} cp_t + \delta_{cpcp} \omega_{cp,t+1},\ cn_{t+1} = cn_0 + \rho_{cncn} cn_t + \delta_{cncn} \omega_{cn,t+1}. \tag{14}$$

The level shocks enter the uncertainty processes to capture the possibility that large positive (negative) growth shocks today indicate more "good" ("bad") future uncertainty. In addition, the asymmetric nature of gamma shocks flexibly introduces non-linearity into uncertainty.

The risk aversion state variable, $q_t = \ln(Q_t)$, evolves over time with a state-dependent persistent conditional mean and a disturbance that is exposed to economic fundamental shocks. The residual is then separated into two independent gamma shocks, $\omega_{qp,t+1}$ and $\omega_{qn,t+1}$, to capture the possibly asymmetric behaviors of the right-tail (more risk averse) and left-tail (less risk averse) preference shocks:

$$\begin{aligned} q_{t+1} = q_0 + \rho_q q_t + \rho_{qcp} cp_t + \rho_{qcn} cn_t + \rho_{qqp} qp_t + \rho_{qqn} qn_t \\ + \delta_{qcp} \omega_{cp,t+1} + \delta_{qcn} \omega_{cn,t+1} + \delta_{qqp} \omega_{qp,t+1} - \delta_{qqn} \omega_{qn,t+1}, \end{aligned} \tag{15}$$

$$\omega_{qp,t+1} = \Gamma(qp_t, 1) - qp_t,\ \omega_{qn,t+1} = \Gamma(qn_t, 1) - qn_t, \tag{16}$$

where qp_t and qn_t are shape parameters of the two risk aversion shocks, respectively, and are assumed with isomorphic dynamics processes:

$$qp_{t+1} = qp_0 + \rho_{qpqp} qp_t + \delta_{qpqp} \omega_{qp,t+1},\ qn_{t+1} = qn_0 + \rho_{qnqn} qn_t + \delta_{qnqn} \omega_{qn,t+1}. \tag{17}$$

We motivate this reduced-form risk aversion process as follows. First, the conditional mean of q_{t+1} is driven by past states of both economic fundamentals and risk aversion, which is consistent with recent micro-level evidence, such as in Malmendier and Nagel (2011). Second, allowing contemporaneous fundamental shocks to span the risk aversion process is consistent with Campbell and Cochrane (1999), while allowing for a non-fundamental source of risk aversion is consistent with the evidence presented in Bekaert, Engstrom, and Xu (2020), who find that risk aversion filtered from risky asset prices contains a pure preference component that is crucial in explaining various non-linear asset moments. Third, different from the risk aversion process in Bekaert, Engstrom, and Xu (2020), our risk aversion process allows different and asymmetric dynamics for the upside and downside preference shocks, which is a realistic assumption as evidence suggests that there is a higher chance of observing extreme large risk

aversion than extreme low risk aversion (see e.g. a lab experiment in Ebert (2015)).

Finally, the aggregate dividend growth has a similar dynamic process featuring asymmetric fundamental shock exposures and upside and downside dividend-specific shocks:

$$\Delta d_{t+1} = d_0 + \rho_{dcp} cp_t + \rho_{dcn} cn_t + \delta_{dcp}\omega_{cp,t+1} + \delta_{dcn}\omega_{cn,t+1} + \delta_{ddp}\omega_{dp,t+1} - \delta_{ddn}\omega_{dn,t+1}, \quad (18)$$

where the upside ($\omega_{dp,t+1}$) and downside ($\omega_{dn,t+1}$) cash flow shocks are centered homoskedastic gamma shocks for the purpose of simplicity without changing the model implications.[9] The cash flow shocks are assumed to be independent from the preference shocks.

Hence, we can summarize the global state variables using a linear matrix representation as follows:

$$\boldsymbol{Y_{t+1}} = \boldsymbol{\mu} + \boldsymbol{A}\boldsymbol{Y_t} + \boldsymbol{\Sigma}\boldsymbol{\omega_{t+1}}, \quad (19)$$

where $\boldsymbol{Y_{t+1}}$ (7-by-1) contains $\{\Delta c_{t+1}, q_{t+1}, \Delta d_{t+1}, cp_{t+1}, cn_{t+1}, qp_{t+1}, qn_{t+1}\}$; $\boldsymbol{\omega_{t+1}}$ (6-by-1) contains six centered independent gamma shocks $\{\omega_{cp,t+1}, \omega_{cn,t+1}, \omega_{qp,t+1}, \omega_{qn,t+1}, \omega_{dp,t+1}, \omega_{dn,t+1}\}$; and $\boldsymbol{\Sigma}$ is a 7-by-6 matrix. The shock assumption of the centered, mutually independent $\boldsymbol{\omega_{t+1}}$ can be generalized into $\boldsymbol{\omega_{t+1}} \sim \Gamma(\boldsymbol{\Omega}\boldsymbol{Y_t} + \boldsymbol{e}, 1) - (\boldsymbol{\Omega}\boldsymbol{Y_t} + \boldsymbol{e})$, where $\boldsymbol{\Omega}$ is a 6-by-7 matrix and $\boldsymbol{e}$ a 6-by-1 matrix to capture constant shape parameters.[10]

4.2. The world economy

Next, we model the international counterparts: country pricing kernels and state variables. We assume that country i has a representative investor who has a period utility function as follows:

$$U(C_t^i) = \frac{(C_t^i/Q_t^i)^{1-\gamma}}{1-\gamma}, \quad (20)$$

where C_t^i is the consumption level and Q_t^i drives the time variation in her RRA. We assume that the consumption and RRA levels follow a power product with a global component and an

[9] Assuming heteroskedastic cash flow shocks does not change the model implications for the dynamics of VP. This is because "pure" cash flow shocks ($\omega_{dp,t+1}$ and $\omega_{dn,t+1}$) are not correlated with kernel shocks and thus are not compensated.

[10] To be more specific, $\boldsymbol{\Omega} = \begin{bmatrix} 0 & 0 & 0 & 1 & 0 & 0 & 0 \\ 0 & 0 & 0 & 0 & 1 & 0 & 0 \\ 0 & 0 & 0 & 0 & 0 & 1 & 0 \\ 0 & 0 & 0 & 0 & 0 & 0 & 1 \\ 0 & 0 & 0 & 0 & 0 & 0 & 0 \\ 0 & 0 & 0 & 0 & 0 & 0 & 0 \end{bmatrix}$, $\boldsymbol{e} = \begin{bmatrix} 0 & 0 & 0 & 0 & \overline{dp} & \overline{dn} \end{bmatrix}'$, where $\overline{dp}$ ($\overline{dn}$) is the constant shape parameter of the upside (downside) cash flow shock, $\omega_{dp,t+1}$ ($\omega_{dn,t+1}$).

idiosyncratic component that are log-linearly weighted by constant parameters α^i's:

$$C_t^i = (C_t)^{\alpha_1^i} \left(C_t^{i,f}\right)^{1-\alpha_1^i}, \tag{21}$$

$$Q_t^i = (Q_t)^{\alpha_2^i} \left(Q_t^{i,f}\right)^{1-\alpha_2^i}, \tag{22}$$

where C_t and Q_t are defined in Section 4.1; $C_t^{i,f}$ and $Q_t^{i,f}$ denote country-specific counterparts.[11] Hence, changes in consumption, $\Delta c_{t+1}^i \equiv \ln(C_{t+1}^i/C_t^i)$, can be written as $\alpha_1^i \Delta c_{t+1} + (1-\alpha_1^i)\Delta c_{t+1}^{i,f}$; similarly, $q_{t+1}^i \equiv \ln(Q_{t+1}^i) = \alpha_2^i q_{t+1} + (1-\alpha_2^i) q_{t+1}^{i,f}$.

Foreign country i investor's intertemporal marginal rate of substitution is given by $M_{t+1}^i = \beta^i \frac{U'(C_{t+1}^i)}{U'(C_t^i)} = \beta^i \frac{(C_{t+1}^i/Q_{t+1}^i)^{-\gamma}}{(C_t^i/Q_t^i)^{-\gamma}}$, and the logarithm of her SDF follows:

$$m_{t+1}^i = \ln(\beta^i) - \gamma\alpha_1^i \Delta c_{t+1} - \gamma(1-\alpha_1^i)\Delta c_{t+1}^{i,f} + \gamma\alpha_2^i \Delta q_{t+1} + \gamma(1-\alpha_2^i)\Delta q_{t+1}^{i,f}, \tag{23}$$

which, intuitively, contains global and idiosyncratic parts. Parameters α^i's hence can be interpreted as integration coefficients, as they characterize country i's exposures to the common shocks through a real economic channel (α_1^i) and a risk aversion channel (α_2^i).

For the dynamic processes of country i's consumption, risk aversion, and cash flow (dividend growth), we assume that state variables follow a similar linear structure that contains global and idiosyncratic parts:

$$\boldsymbol{Y_{t+1}^i} = \boldsymbol{B^i Y_{t+1}} + (\mathbf{1} - \boldsymbol{B^i})\boldsymbol{Y_{t+1}^{i,f}}, \tag{24}$$

where $\boldsymbol{Y_{t+1}}$ is a vector of global state variables (including second moments) as defined in Equation (19) and $\boldsymbol{B^i}$ summarizes the global exposures. The idiosyncratic counterpart $\boldsymbol{Y_{t+1}^{i,f}}$ is assumed with a similar vector autoregressive structure:

$$\boldsymbol{Y_{t+1}^{i,f}} = \boldsymbol{\mu^{i,f}} + \boldsymbol{A^{i,f}} \boldsymbol{Y_t^{i,f}} + \boldsymbol{\Sigma^{i,f}} \boldsymbol{\omega_{t+1}^{i,f}}, \tag{25}$$

where $\boldsymbol{\mu^{i,f}}$ and $\boldsymbol{A^{i,f}}$ are constant matrices and $\boldsymbol{\omega_{t+1}^{i,f}}$ denotes a vector of idiosyncratic shocks that also follow centered gamma distributions. We do not need to explicitly impose distributional assumptions on these idiosyncratic shocks because our goal is to use the framework to rationalize the dynamic behaviors and international predictability patterns of the asymmetric global risk variables (our main empirical findings).

[11] The curvature parameter γ can also be generalized to be country-specific, which would be reflected in the model solution as an additional source of heterogeneity across countries.

4.3. Relevant model solution

We first derive the model solution for the U.S. VP using the U.S. pricing kernel and state variables and then the solution for the international equity risk premiums using their country counterparts. Given the Euler equation with the no-arbitrage assumption and the MGF of the sum of gamma shocks, this model fits into the exponential affine class. Thus, the model solution for the risk free rate, valuation ratio, equity risk premium, and higher-order moments of equity returns can be shown to be (approximately) linear to $\boldsymbol{Y_t}$ and $\boldsymbol{Y_t^{i,f}}$.

A. The U.S. variance risk premium: The log global pricing kernel can be rewritten as follows,

$$m_{t+1} = m_0 + \boldsymbol{m_1 Y_t} + \boldsymbol{m_2 \Sigma \omega_{t+1}}, \tag{26}$$

where $\boldsymbol{Y_t}$, $\boldsymbol{\omega_{t+1}}$, and $\boldsymbol{\Sigma}$ are introduced in Equation (19), and $\boldsymbol{m_1}$ (1-by-7) and $\boldsymbol{m_2}$ (1-by-7) are vectors of kernel loadings on lagged state variables and shocks, respectively. Given the assumptions on the utility function and state variable dynamics (Section 4.1), the U.S. pricing kernel receives four shocks per period: two real macro shocks capturing asymmetric economic growth uncertainties, $\{\omega_{cp,t+1}, \omega_{cn,t+1}\}$, and two non-fundamental shocks capturing asymmetric tail behaviors of risk aversion, $\{\omega_{qp,t+1}, \omega_{qn,t+1}\}$. By design, these four shocks are orthogonal to each other.

The price-dividend ratio can be solved in an approximate affine framework and log market returns also have a linear expression with constant return sensitivities to these shocks (ignore the approximation error),[12]

$$r_{t+1} = \xi_0 + \boldsymbol{\xi_1 Y_t} + \boldsymbol{\xi_2 \Sigma \omega_{t+1}}, \tag{27}$$

where $\boldsymbol{\xi_1}$ (1-by-7) and $\boldsymbol{\xi_2}$ (1-by-7) are vectors of return loadings on lagged state variables and shocks, respectively. The MGF of log market returns under the risk-neutral measure, $MGF_t^Q(r_{t+1};\nu)$, is $\frac{E_t[\exp(m_{t+1}+\nu r_{t+1})]}{E_t[\exp(m_{t+1})]}$. The risk-neutral conditional variance, $V_t^Q(r_{t+1})$, is $E_t^Q\left(r_{t+1}^2\right) - \left(E_t^Q(r_{t+1})\right)^2$, where both expectations can be derived by taking derivatives of $MGF_t^Q(r_{t+1};\nu)$ and fixing ν at 0. The model-implied U.S. VP has the following expression:

$$\begin{aligned} V_t^Q(r_{t+1}) - V_t^P(r_{t+1}) &= \left\{(\boldsymbol{\xi_2 \Sigma})^{\circ 2} \circ \left[(\mathbf{1} - \boldsymbol{m_2 \Sigma})^{\circ -2} - \mathbf{1}\right]\right\}(\boldsymbol{\Omega Y_t} + \boldsymbol{e}) \\ &\equiv DVP + UVP, \end{aligned} \tag{28}$$

[12] See Appendix A for proof.

where "$\circ$" indicates element-by-element matrix multiplication.

Here are some insights from Equation (28). The dynamics of VP (and its components) are driven by the four premium state variables $\{cp_t, cn_t, qp_t, qn_t\}$, given that the kernel loads on the four shocks (ω_{cp}, ω_{cn}, ω_{qp}, and ω_{qn}). Given the sandwich form and the strictly positive nature of the shape parameters, it is crucial to understand the sign of $\left[(\mathbf{1} - \boldsymbol{m_2\Sigma})^{\circ -2} - \mathbf{1}\right]$ with respect to each premium state variable. In the model, the pricing kernel generally increases with risk aversion and decreases with consumption growth. Therefore, m_{t+1} likely loads positively on both the right-tail or upside risk aversion shock (ω_{qp}) and the left-tail or downside real shock (ω_{cn}), or $m_2(\omega_{qp}) > 0$ and $m_2(\omega_{cn}) > 0$; both shocks are likely to spike up in a bad environment. With positive m loadings, $\left[\left(\frac{1}{1-m_2\sigma}\right)^2 - 1\right] > 0$, which renders a strictly higher compensation demanded for variance risk when risk aversion or real downside uncertainty increases. On the other hand, the other two shocks, the upside real shock ω_{cp} and left-tail swings in risk aversion ω_{qn}, likely have negative kernel loadings; for instance, good economic uncertainty due to growth spurts might contribute negatively to VP, as the kernel likely decreases with growth spurts or $m_2(\omega_{cp}) < 0$. Therefore, the closed-form solution in Equation (28) has the potential to suggest economic sources of the VP components.

B. The U.S. equity risk premium: The U.S. equity risk premium can be derived as follows:

$$E_t(r_{t+1}) - rf_t = \{\boldsymbol{\xi_2\Sigma} + \ln\left[\mathbf{1} - (\boldsymbol{m_2} + \boldsymbol{\xi_2})\boldsymbol{\Sigma}\right] - \ln(\mathbf{1} - \boldsymbol{m_2\Sigma})\}\,(\boldsymbol{\Omega Y_t} + \boldsymbol{e}), \tag{29}$$

where the relevant state variables in $\boldsymbol{Y_t}$ that drive the time variation in the U.S. equity risk premium are the four premium state variables $\{cp_t, cn_t, qp_t, qn_t\}$. To gain intuition, its Gaussian approximation contains the risk compensation term $-\,(\boldsymbol{m_2\Sigma} \circ \boldsymbol{\xi_2\Sigma})\,(\boldsymbol{\Omega Y_t} + \boldsymbol{e})$, or $-Cov_t(r_{t+1}, m_{t+1})$. Only return exposures to kernel shocks are compensated to the U.S. investor. Equity risk premium loadings can also be suggested. For example, the traditional asset pricing literature suggests that investors demand higher risk compensation given higher risk aversion; in our model, the coefficient of the right-tail of risk aversion qp_t in the equity risk premium is indeed positive because $m_2(qp) > 0$ (i.e., higher risk aversion drives up the marginal utility) and $\xi_2(qp) < 0$ (i.e., through both the interest rate and the compensation channels).

C. International equity risk premiums: Country i's equity risk premium can be derived as follows:

$$E_t(r^i_{t+1}) - rf^i_t = \left\{ \boldsymbol{\xi_2^i \Sigma} + \ln\left[\mathbf{1} - (\boldsymbol{m_2^i} + \boldsymbol{\xi_2^i})\boldsymbol{\Sigma}\right] - \ln(\mathbf{1} - \boldsymbol{m_2^i \Sigma}) \right\} (\boldsymbol{\Omega Y_t} + \boldsymbol{e}) \qquad (30)$$
$$+ \text{Idiosyncratic component},$$

where, similarly, $\boldsymbol{\xi_2^i}$ denotes the sensitivity of country i's log market returns to global shocks and $\boldsymbol{m_2^i}$ denotes the sensitivity of country i's log pricing kernel to global shocks; $\boldsymbol{\Sigma}$, $\boldsymbol{\Omega}$, $\boldsymbol{Y_t}$, and $\boldsymbol{e}$ are implied from Equation (19). Similarly, a Gaussian approximation of the global part of international equity risk premiums above contains a global compensation component, $-\left(\boldsymbol{m_2^i \Sigma} \circ \boldsymbol{\xi_2^i \Sigma}\right)(\boldsymbol{\Omega Y_t} + \boldsymbol{e})$, or $-Cov_t(r^i_{t+1}, m_{t+1})$.

The first observation is that global shocks are priced in country equities as they enter both the comoving local pricing kernel and cash flow processes through the integration assumptions. Second, global premium state variables determine the time variation in international equity premiums, and different country sensitivities to global shocks play an important role in explaining the cross-country variation in the global part of the country equity risk premiums. Third, the global premium state variables, $\{cp_t, cn_t, qp_t, qn_t\}$, drive both the time variation in the U.S. VP (and thus its components), according to Equation (28), and international equity risk premiums. Hence, the model solution sheds light on the international stock return predictability of VP and its components.

4.4. Estimation strategy and results

To maintain the empirical focus of the paper, we propose a parsimonious three-step estimation approach to bring our model solution to the data. The goal is to explain the distinct dynamic behaviors and international predictability patterns of DVP and UVP within a consistent asset pricing framework, as established in Sections 2 and 3. We first estimate the four global premium state variables in Section 4.4.1. Then, in Section 4.4.2, we estimate separate loadings of DVP and UVP on the global premium state variables by jointly matching empirical estimates of DVP and UVP. Finally, in Section 4.4.3, we use empirical estimates of international predictive coefficients of DVP and UVP at various horizons to identify the relative importance of global premium state variables in driving the global part of international equity premiums.

4.4.1. Estimating the U.S. premium state variables

Given the data availability and timely releases, we follow the empirical macro literature (e.g., Jurado, Ludvigson, and Ng (2015)) and use the log U.S. industrial production growth (denoted by θ_t; source: FRED) as the empirical proxy for our main real macro variable. We use Bates (2006)'s approximate MLE methodology to estimate real non-Gaussian fundamental shocks ($\omega_{\theta p,t}$, $\omega_{\theta n,t}$) and uncertainty state variables (θp_t, θn_t), using the longest sample available, which runs from January 1947 to March 2018. Detailed estimation results are reported in Table B1 of the Appendix. The two plots of Figure 10 depict the time series of θp_t and θn_t, respectively. Given that a lower shape parameter indicates less Gaussainity (i.e., statistical property of a gamma distribution), these two plots suggest that the left tail of the real growth rates are more non-Gaussian and left-skewed. In addition, the upside uncertainty state variable θp_t appears more persistent ($\rho_{\theta p}$=0.99***) than the downside uncertainty state variable θn_t ($\rho_{\theta n}$=0.95***). We find that θn_t is countercyclical, as it comoves positively with the NBER recession indicator (ρ=0.60***), whereas θp_t appears acyclical. It is noteworthy that the magnitudes of these uncertainty state variables are not the magnitudes of uncertainties because the actual conditional variance of economic growth includes the scale parameters, $Var_t(\theta_{t+1}) = \delta_{\theta\theta p}\theta p_t + \delta_{\theta\theta n}\theta n_t$. Given our scale parameter estimates, the downside uncertainty $\delta_{\theta\theta n}\theta n_t$ explains an average of 89% (67%) of the total variance during recessions (normal periods).

Next, we filter our risk aversion state variables (qp_t, qn_t) from the risk aversion measure constructed by Bekaert, Engstrom, and Xu (2020). One important feature of their q_t measure is that it is also motivated from an external habit formation model; in addition, their q_t measure is filtered from a wide set of financial and economic data while satisfying pricing consistency in the market and thus is suitable for our research to maintain the empirical focus of our paper.[13] Different from their objective, our framework allows for separate tail dynamics of downside and upside preference shocks to capture a non-fundamental source of *asymmetry*. The estimation uses the Bates (2006) methodology and the longest available sample (starting from June 1986); detailed estimation results can be found in Table B2 of the Appendix.

The last two plots of Figure 10 demonstrate that the pure right-tail risk aversion state variable qp_t — capturing the right-tail variability of risk aversion after controlling for responses

[13]It is widely agreed that q_t filtered from standard habit formation process (such asCampbell and Cochrane (1999) and Wachter (2006)) is unrealistically persistent with a monthly AR(1) coefficient around 0.995.

to changes in fundamentals — exhibits substantial time variation, which stands in sharp contrast to the behavior of the pure left-tail risk aversion state variable qn_t. That is, it is more likely to see extreme fluctuations in the high risk aversion domain. To formalize this observation, the persistent coefficient of qp_t is 0.64*** while that of qn_t is close to 1. The level of qp_t (around 14.59***) is significantly smaller than that of qn_t (around 612.32***), suggesting that the right tail of risk aversion accounts for most of the non-Gaussian properties of the total pure risk aversion. Finally, qp_t (qn_t) is tested to be countercyclical (procyclical), indicating a higher chance of observing extreme high (low) risk aversion realizations during recessions (normal periods). Our evidence further suggests that separating the tail behaviors of time-varying risk aversion is potentially important as the pure downside (left-tail) and upside (right-tail) risk aversion shocks account for 8% and 72% of the total risk aversion variability.[14]

4.4.2. Decomposing the Dynamics of DVP and UVP

The second step aims to identify the loadings of DVP and UVP on the four global premium state variables by matching their estimated empirical dynamics. We construct a GMM system. For each iteration, we compute the model-implied DVP and UVP, denoted by $\widehat{vp_t^D}$ and $\widehat{vp_t^U}$, respectively, given the loading parameter candidates, denoted by w:

$$\begin{aligned}\widehat{vp_t^D} &= w^D_{\theta p,t}\widehat{\theta p}_t + w^D_{\theta n,t}\widehat{\theta n}_t + w^D_{qp,t}\widehat{qp}_t + w^D_{qn,t}\widehat{qn}_t,\\ \widehat{vp_t^U} &= w^U_{\theta p,t}\widehat{\theta p}_t + w^U_{\theta n,t}\widehat{\theta n}_t + w^U_{qp,t}\widehat{qp}_t + w^U_{qn,t}\widehat{qn}_t,\end{aligned} \tag{31}$$

where $\forall x \in \{\theta p, \theta n, qp, qn\}$, the time-varying coefficients are linearly spanned by a common economic indicator z_t:

$$w^D_{x,t} = w^D_{x,0} + w^D_{x,1}z_t,\ w^U_{x,t} = w^U_{x,0} + w^U_{x,1}z_t. \tag{32}$$

We choose the squared real growth innovation as an appropriate proxy of z_t inspired by the realized variance literature. In addition, the right-skewed nature of z_t introduces exogenous non-linearity for reasons beyond the present modeling framework.[15] Hence, there are 16 unknown parameters in this GMM system, $\boldsymbol{w} = \{w^D_{\theta p,0},\ w^D_{\theta n,0},\ w^D_{qp,0},\ w^D_{qn,0},\ w^U_{\theta p,0},\ w^U_{\theta n,0},\ w^U_{qp,0},\ w^U_{qn,0},\ w^D_{\theta p,1},\ w^D_{\theta n,1},\ w^D_{qp,1},\ w^D_{qn,1},\ w^U_{\theta p,1},\ w^U_{\theta n,1},\ w^U_{qp,1},\ w^U_{qn,1}\}$.

Denote the empirical estimates of the one-month-ahead VP components in Section 2 as $\widetilde{vp_t^D}$ and $\widetilde{vp_t^U}$. The orthogonality conditions $E[\boldsymbol{\varepsilon}(\boldsymbol{w}|\Psi_t)] = \mathbf{0}$ are determined as follows:

[14] More details are provided in Figure iv of the Internet Appendix.

[15] For instance, David and Veronesi (2013) show a Bayesian learning story where asset prices and moments can be more sensitive to risk variables after bad news as investors take time to learn.

$$\varepsilon(\boldsymbol{w}|\Psi_t) = \begin{bmatrix} \widetilde{vp_t^D} - \widehat{vp_t^D} \\ \widetilde{vp_t^U} - \widehat{vp_t^U} \\ \left(\widetilde{vp_t^D} - E(\widetilde{vp_t^D})\right)^2 - \left(\widehat{vp_t^D} - E(\widehat{vp_t^D})\right)^2 \\ \left(\widetilde{vp_t^U} - E(\widetilde{vp_t^U})\right)^2 - \left(\widehat{vp_t^U} - E(\widehat{vp_t^U})\right)^2 \\ \frac{\left(\widetilde{vp_t^D} - E(\widetilde{vp_t^D})\right)^3}{Var(\widetilde{vp_t^D})^{3/2}} - \frac{\left(\widehat{vp_t^D} - E(\widehat{vp_t^D})\right)^3}{Var(\widehat{vp_t^D})^{3/2}} \\ \frac{\left(\widetilde{vp_t^U} - E(\widetilde{vp_t^U})\right)^3}{Var(\widetilde{vp_t^U})^{3/2}} - \frac{\left(\widehat{vp_t^U} - E(\widehat{vp_t^U})\right)^3}{Var(\widehat{vp_t^U})^{3/2}} \\ \frac{\left(\widetilde{vp_t^D} - E(\widetilde{vp_t^D})\right)^4}{Var(\widetilde{vp_t^D})^2} - \frac{\left(\widehat{vp_t^D} - E(\widehat{vp_t^D})\right)^4}{Var(\widehat{vp_t^D})^2} \\ \frac{\left(\widetilde{vp_t^U} - E(\widetilde{vp_t^U})\right)^4}{Var(\widetilde{vp_t^U})^2} - \frac{\left(\widehat{vp_t^U} - E(\widehat{vp_t^U})\right)^4}{Var(\widehat{vp_t^U})^2} \\ \left(\widetilde{vp_t^D} - E(\widetilde{vp_t^D})\right)\left(\widetilde{vp_t^U} - E(\widetilde{vp_t^U})\right) - \left(\widehat{vp_t^D} - E(\widehat{vp_t^D})\right)\left(\widehat{vp_t^U} - E(\widehat{vp_t^U})\right) \\ \frac{\widetilde{vp_t^D}}{\widetilde{vp_t^D} + \widetilde{vp_t^U}} - \frac{\widehat{vp_t^D}}{\widehat{vp_t^D} + \widehat{vp_t^U}} \end{bmatrix}, \tag{33}$$

where Ψ_t represents the information set of month t consisting of $\{\widehat{\theta p}_t, \widehat{\theta n}_t, \widehat{qp}_t, \widehat{qn}_t, \widehat{vp_t^D}, \widehat{vp_t^U}\}$ and z_t; the model-implied VP components, $\widehat{vp_t^D}$ and $\widehat{vp_t^U}$, contain the unknown parameters $\boldsymbol{w}$; the raw moment conditions of interest include mean (2 moments), variance (2), scaled skewness (2), scaled kurtosis (2), covariance (1), and fraction of DVP in VP (1). Each raw moment condition is then tensor-multiplied with a set of instruments $\{1, \widehat{\theta p}_t, \widehat{\theta n}_t, \widehat{qp}_t, \widehat{qn}_t, \theta_{t-1}, q_{t-1}, u_{\theta,t}, u_{q,t}\}$ including the real growth innovation $u_{\theta,t}$ and the risk aversion innovation $u_{q,t}$. The GMM system has 90 moments and 16 unknowns and is estimated using iterative GMM.

Table 8 presents the moment matching results of the GMM system. Panel A shows that all moments are significantly close to their empirical counterparts. Panel B shows that we fail to reject Hansen's J test, indicating that these over-identification restrictions/moments are valid. Given the non-Gaussian nature of the VP components, a simple (Pearson's) correlation coefficient only provide suggestive evidence of the dynamic fit. Figure 11 shows that our model-implied DVP is highly correlated with its empirical counterpart with a correlation coefficient of 0.56. Matching the dynamics of UVP is admittedly more difficult because UVP is a more transitory variable. We are able to match some major drops of UVP during key episodes in 2008 and 2012.[16]

Next, we discuss the relative importance of the four premium state variables in explaining the dynamics of the model-implied DVP and UVP. Panel A of Table 9 shows that DVP loads strongly and positively on right-tail movements of risk aversion, captured by state variable qp_t.

[16]We have also estimated the same GMM system with constant loadings (i.e., $w^i_{x,1} = 0$, for $i = D, U$, in Equation (32)). The results for this specification are strictly weaker in terms of the matching; a time-series comparison can be found in Figure v of the Internet Appendix.

According to the variance decomposition results (henceforth "VARC"), qp_t accounts for most (41.37% of which 39.97% come from the constant loading and 1.4% from the time-varying loading) of the dynamics of DVP. The significant and positive estimate of w_1 (159.57***) suggests that DVP responds to qp more strongly during environments with high current real economic fluctuations. As an interpretation of these findings, investors are willing to pay extra to buy protection against bad variance risk when risk aversion is high; moreover, they are willing to pay more when they observe higher current real economic fluctuations.

To offer some economic magnitudes of the loadings, Panel B of Table 9 calculates the loadings at various values of z_t. Because z_t is an extremely right-skewed variable and is always greater than 0, we consider the mean and two extreme right-tail values (90th and 95th). For DVP, one standard deviation (SD) increase in the right-tail risk aversion state variable qp_t is associated with the highest marginal increases at all three z_t values; consistent with Panel A, the effect of qp_t increases as investors observe more extreme real fluctuations in the economy (i.e., from 8.54 to 8.81 monthly percentage squared). DVP also increases when downside economic uncertainty is higher in general: one SD increase in θn_t could cause DVP to increase by 6 monthly percentage squared at the average z_t. However, DVP responds less to economic uncertainty during extremely volatile business conditions, as the positive θn_t effect becomes smaller as z_t increases.

UVP is more sensitive to economic uncertainty, given the variance decomposition and loading evidence from, respectively, Panels A and B of Table 9. In particular, the loading of UVP on one SD change in θn_t is the strongest across all other state variables and for all business conditions of z_t. The loading is more negative under environments with high real growth fluctuations. One SD increase in downside uncertainty results in mild drops in UVP of 1.77 monthly percentage squared when realized economic variance is at its historical average, which is followed by extremely large drops in UVP when realized economic variance starts to increase (around 7.61 at its 95th percentile and 29.12 at its 99th percentile). It is noteworthy that the historical standard deviation of UVP is only 3.77 monthly percentage squared.

The analysis in this section sheds light on the empirical findings established in Section 2. In particular, UVP loads primarily and negatively on the countercyclical downside uncertainty (θn_t) while DVP loads primarily and positively on the countercyclical risk aversion variability (qp_t). This renders a procyclical UVP and a countercyclical DVP. In addition, while the loading of DVP on its main determinant is relatively stable at various business conditions, that of UVP

on its main determinant deepens quickly as the environment becomes more volatile. This is consistent with the finding that UVP is more transitory than DVP.

4.4.3. Understanding the international return predictability patterns

Our model solution suggests that the four global premium state variables drive VP and international equity risk premiums in equilibrium, and thus account for international return predictability of the VP components. In this step, we infer loadings of international equity risk premiums on these global state variables over different horizons such that the distances between model-implied predictive coefficients and their empirical counterparts (obtained from Section 3) are minimized.

From Section 4.3, the one-month-ahead country equity risk premium has a global part that linearly spans the four global premium state variables. Because these four global premium state variables follow AR(1) processes, the expectation of h-month-ahead excess returns, $\widehat{ERP}^i_{h,t}$, can also be written as a linear combination of real uncertainty and risk aversion state variables:

$$\begin{aligned}\widehat{ERP}^i_{h,t} = v^i_{\theta p,h,t}\widehat{\theta p}_t + v^i_{\theta n,h,t}\widehat{\theta n}_t + v^i_{qp,h,t}\widehat{qp}_t + v^i_{qn,h,t}\widehat{qn}_t \\ + \text{idiosyncratic component},\end{aligned} \tag{34}$$

where the four empirical proxies for the state variables, $\widehat{\theta p}_t$, $\widehat{\theta n}_t$, $\widehat{qp}_t$, and $\widehat{qn}_t$, are estimated and discussed in Section 4.4.1. The loadings are assumed as follows:

$$\begin{aligned} v^i_{\theta p,h,t} &= v_{\theta p,h,0} + \boldsymbol{v_{\theta p,h,1}}' \boldsymbol{x^i} + v_{\theta p,h,2} z_t, \\ v^i_{\theta n,h,t} &= v_{\theta n,h,0} + \boldsymbol{v_{\theta n,h,1}}' \boldsymbol{x^i} + v_{\theta n,h,2} z_t, \\ v^i_{qp,h,t} &= v_{qp,h,0} + \boldsymbol{v_{qp,h,1}}' \boldsymbol{x^i} + v_{qp,h,2} z_t, \\ v^i_{qn,h,t} &= v_{qn,h,0} + \boldsymbol{v_{qn,h,1}}' \boldsymbol{x^i} + v_{qn,h,2} z_t, \end{aligned} \tag{35}$$

where $\boldsymbol{x^i}$ is a set of country-specific variables that are potentially informative about the cross-country differences of international equity risk premium loadings on the global premium variables. Due to the potential large number of unknown parameters to be estimated when including many country-specific characteristics, we focus on two country integration indicators. We use the 1989-2017 averages of credit-to-GDP ratio (source: BIS) to capture financial integration and trade-to-GDP ratio (source: World Bank) to capture real/economic integration; $\boldsymbol{x^i}$ uses the standardized values for interpretation purpose. As in Equation (32), z_t is the squared real economic growth innovation.

The model-implied h-month predictive coefficient of DVP for country i is thus given by:

$$\widehat{b^i_{h,D}} \equiv \frac{Cov(\widehat{vp^D_t}, \widehat{ERP^i_{h,t}})}{Var(\widehat{vp^D_t})} = \left(\begin{bmatrix} v_{\theta p,h,0} + \boldsymbol{v_{\theta p,h,1}}' \boldsymbol{x^i} \\ v_{\theta n,h,0} + \boldsymbol{v_{\theta n,h,1}}' \boldsymbol{x^i} \\ v_{qp,h,0} + \boldsymbol{v_{qp,h,1}}' \boldsymbol{x^i} \\ v_{qn,h,0} + \boldsymbol{v_{qn,h,1}}' \boldsymbol{x^i} \\ v_{\theta p,h,2} \\ v_{\theta n,h,2} \\ v_{qp,h,2} \\ v_{qn,h,2} \end{bmatrix}' \boldsymbol{\Xi} \begin{bmatrix} w^D_{\theta p,0} \\ w^D_{\theta n,0} \\ w^D_{qp,0} \\ w^D_{qn,0} \\ w^D_{\theta p,1} \\ w^D_{\theta n,1} \\ w^D_{qp,1} \\ w^D_{qn,1} \end{bmatrix} \right) / \left(\begin{bmatrix} w^D_{\theta p,0} \\ w^D_{\theta n,0} \\ w^D_{qp,0} \\ w^D_{qn,0} \\ w^D_{\theta p,1} \\ w^D_{\theta n,1} \\ w^D_{qp,1} \\ w^D_{qn,1} \end{bmatrix}' \boldsymbol{\Xi} \begin{bmatrix} w^D_{\theta p,0} \\ w^D_{\theta n,0} \\ w^D_{qp,0} \\ w^D_{qn,0} \\ w^D_{\theta p,1} \\ w^D_{\theta n,1} \\ w^D_{qp,1} \\ w^D_{qn,1} \end{bmatrix} \right), \tag{36}$$

where $\boldsymbol{\Xi}$ is the covariance-variance matrix of $\begin{bmatrix} \theta p_t & \theta n_t & qp_t & qn_t & \theta p_t z_t & \theta n_t z_t & qp_t z_t & qn_t z_t \end{bmatrix}$. A similar calculation applies to the UVP predictive coefficients $\widehat{b^i_{h,U}}$; all w parameters are obtained from Step 2 in Section 4.4.2. For each horizon h, there are 16 unknown parameters,[17] and the estimation is conducted by minimizing the sum of squared standardized residuals for 22 $\widehat{b^i_{h,D}}$, 22 $\widehat{b^i_{h,U}}$, and the unconditional h-month-ahead U.S. equity risk premium.[18] As a result, the estimation results reconcile both DVP and UVP predictive patterns for all countries. Finally, it is unclear how to jointly explain all predictive coefficients across all horizons without certain parametric assumptions. As a result, we estimate the system for each horizon separately.

Tables 10 and 11 provide the coefficient matching for the U.S. and for the panel of countries, respectively. We find that model-implied predictive coefficients are statistically close to their empirical counterparts.

We then evaluate the economic significance of each of the four global premium state variables, $\{\theta p, \theta n, qp, qn\}$, in explaining the international predictability patterns. To do so, we conduct a "Jackknife"-type exercise for each horizon. Specifically, we "delete" one state variable at a time by setting all v loadings associated with the state variable to be 0 and recalculate the implied predictive coefficient without re-estimation.[19] Table 12 reports the relative changes in the predictive coefficients after deleting a state variable at a time for an average country (average financial and economic integration levels, or $\boldsymbol{x^i} = \boldsymbol{0}$): the more negative the relative change is, the more significant the state variable is in explaining the predictive patterns, given that both DVP and UVP are positive predictors. We focus on horizons between 2 and 7 months

[17] $\boldsymbol{v} = \{v_{\theta p,h,0}, v_{\theta n,h,0}, v_{qp,h,0}, v_{qn,h,0}, \boldsymbol{v_{\theta p,h,1}}, \boldsymbol{v_{\theta n,h,1}}, \boldsymbol{v_{qp,h,1}}, \boldsymbol{v_{qn,h,1}}, v_{\theta p,h,2}, v_{\theta n,h,2}, v_{qp,h,2}, v_{qn,h,2}\}$.

[18] There is no idiosyncratic component for the U.S. equity risk premium.

[19] The reason why we do not re-estimate the system is to ensure a valid comparison with the full model; we expect non-zeros at the off-diagonal terms in $\boldsymbol{\Xi}$ (from Equation (36)), and hence eliminating a state variable and re-estimating the system could result in different v estimates.

because the predictive coefficients of DVP and UVP are significant for most countries during these horizons (Section 3); the last row reflects the average changes of these target horizons.

To explain the predictability pattern of DVP, state variable qp_t — capturing extreme global risk aversion variability — is associated with the most economically significant and statistically negative changes in the international predictability of DVP, according to the left panel of Table 12. The average relative decrease in the DVP predictive coefficient is -4.12 during the target horizons, which is the most negative number in the same row. Hence, the predictability of DVP is mostly explained by the positive loading of international ERPs on global risk aversion, and the risk aversion effect peaks around mid horizons. Figure 12 displays implied term structures of ERP loadings on standardized state variables. The hump-shaped loadings of international ERPs on global risk aversion, according to the red solid line in the "qp" plot (third row of this figure), is consistent with the hump-shaped predictability pattern of DVP.

The right panel of Table 12 shows that deleting the downside uncertainty state variable θn_t dampens the UVP predictive coefficient the most. From Section 4.4.2, we learn that UVP decreases with expected downside economic uncertainty, especially during episodes of large economic fluctuations. Hence, to explain the predictability pattern of UVP (positive; decreasing), we find that the implied ERPs would load negatively on the global downside uncertainty at short horizons, as shown by the red solid line in the "θn" plot (second row) of Figure 12.

It is noteworthy that most asset pricing paradigms imply a positive relation between the countercyclical uncertainty/market volatility and equity risk premium. However, there is still weak empirical evidence on their positive relation and scant evidence on the term structure of this relation. In fact, existing research sometimes finds contradicting results.[20] Instead of directly examining this uncertainty-ERP relation, our approach is to retrieve this latent relation and its term structure by incorporating information from the predictability patterns of both DVP and UVP, which, to the best of our knowledge, is new to the literature. From the second row of Figure 12, we find that, at mid-long horizons (after 8–9 months), there is indeed

[20]Merton et al. (1973) implies a positive risk-return relation, as "investors should be compensated for taking risk," which is intuitively advocated by the mainstream representative-agent asset pricing theories since. However, recent empirical analysis suggests that this relation is only clear for long horizons (see, for instance, Bandi and Perron (2008), Jacquier and Okou (2013)). For shorter horizons, the relation is not as conclusive. Brandt and Kang (2004) document a negative relation between realized market risk and returns using GARCH-class models, while Ghysels, Santa-Clara, and Valkanov (2005) and Ludvigson and Ng (2007) find a positive relation, and Baillie and DeGennaro (1990) and Bollerslev and Zhou (2006) document mixed results. In the consumption-based asset pricing literature, only a few papers examine and provide empirical evidence of a possible procyclical equity risk premium. For instance, Duffee (2005) and Xu (forthcoming) directly examine the comovement between stock returns and consumption growth, which represents the time-varying amount of risk in the equity risk premium in such models and find it to be procyclical.

a positive relation between economic uncertainty and equity risk premium; however, at very short horizons, the relation is negative. In contrast, the equity risk premium loadings on risk aversion are always positive, consistently higher than those on economic uncertainty, and land around reasonable values as theories predict at the annual horizons (i.e., one SD increase in risk aversion is associated with 2.5% increase in annual ERP).[21]

Finally, we discuss the possible transmission/integration channels of global premium state variables to international equity risk premiums, as implied from our estimation. Parameter v_1's in Equation (35) introduce cross-country heterogeneity in predictability coefficients, which, in our estimation setup, is driven by each country's financial and economic integration levels. We conduct a similar Jackknife-exercise using countries with various degrees of financial and economic integration levels. In particular, we denote a country with a trade-to-GDP ratio that is one SD above the world average and an average credit-to-GDP (i.e., more economically integrated) by (1,0), and vice versa.

Table 13 summarizes the average changes in international predictive coefficients between 2- and 7-month horizons after deleting one premium state variable: an average country (as also shown in Table 12), (0,0); a more economically-integrated country, (1,0); and a more financially-integrated country, (0,1).[22] The first main observation is that economic uncertainty becomes more important in explaining the international return predictability of UVP for a more economically-integrated country than for a more financially-integrated country. From the right panel, the average relative drop of the UVP predictive coefficients for horizons of 2 to 7 months is -3.06 for country "(1,0)", which is less than the -1.77 observed for (0,0) and the -2.48 for (0,1). This channel is intuitive as domestic fundamental risk can transmit globally through trade. On the other hand, risk aversion becomes a more significant global premium state variable in explaining the predictability of DVP for a more financially-integrated country than for a more economically-integrated country. From the left panel, the average relative drop of the DVP predictive coefficients for horizons of 2 to 7 months is -13.78 for (0,1), which is less than the -4.12 observed for (0,0) and the -6.06 for (0,1). This result potentially relates to the literature on the importance of financial integration in transmitting investor or effective risk aversion (e.g., Gourinchas and Jeanne (2006), Colacito and Croce (2010), Stiglitz (2010)

[21] Figure vi of the Internet Appendix puts the economic magnitudes of equity risk premium loadings on risk aversion and economic uncertainty in one plot.

[22] Tables v and vi of the Internet Appendix provide exact values for changes in predictive coefficients at all horizons for a more integrated country and a less integrated country. Table 13 reports the averages at horizons 2–7 months.

among many others). As a robustness check, the bottom panel of Table 13 confirms these two observations considering a less integrated country, (-1,0) and (0,-1). As a result, we find that global risk aversion (global economic uncertainty) matters more for explaining stock excess returns in more financially-integrated (economically-integrated) countries. Together with our previous results, DVP (UVP), which is primarily driven by risk aversion (economic uncertainty), transmits to international markets through financial (economic) integration.

5. Conclusion

In this paper, we document and explain the distinct dynamic behaviors and international predictability patterns of U.S. downside and upside variance risk premiums. We find that DVP, the compensation for bearing downside variance risk, is positive, highly correlated with the total variance premium, and countercyclical, whereas UVP is, on average, borderline positive and procyclical with occasional large negative spikes around episodes of market turmoil. We then provide robust evidence that decomposing VP into its downside and upside components significantly improves international stock return predictability for all 22 countries in our sample. The predictive power of DVP peaks at four to six months with a hump-shaped pattern, whereas that of UVP peaks at very short horizons. In the second part of the paper, we rationalize the different dynamic behaviors and international stock return predictability patterns of DVP and UVP in an international no-arbitrage dynamic asset pricing model that features asymmetric shocks and a partially integrated world endowment economy. We first find that DVP is mostly driven by risk aversion, while UVP loads significantly and negatively on downside economic uncertainty; importantly, the sensitivities are amplified when the current economic condition fluctuates more. Then, to jointly explain the predictability patterns of both VP components, we find that the loadings of international equity risk premiums on risk aversion should be positive and hump-shaped, while the loadings on economic uncertainty could be negative at very short horizons but eventually turn positive after 8 months. Hence, we are among the first to uncover the latent relation between uncertainty and equity risk premiums by incorporating information from predictability patterns. Finally, we find that DVP (UVP) likely transmits to international markets through financial integration (real economic integration).

References

Andersen, T. G., Bondarenko, O., 2009. Dissecting the market pricing of return volatility. Working paper .

Baele, L., Driessen, J., Ebert, S., Londono, J. M., Spalt, O., 2018. Cumulative prospect theory, option returns, and the variance premium. The Review of Financial Studies, forthcoming .

Baillie, R. T., DeGennaro, R. P., 1990. Stock returns and volatility. Journal of financial and Quantitative Analysis 25, 203–214.

Bandi, F. M., Perron, B., 2008. Long-run risk-return trade-offs. Journal of Econometrics 143, 349–374.

Bates, D. S., 2006. Maximum likelihood estimation of latent affine processes. The Review of Financial Studies 19, 909–965.

Bekaert, G., Engstrom, E., 2017. Asset return dynamics under habits and bad environmentgood environment fundamentals. Journal of Political Economy 125, 713–760.

Bekaert, G., Engstrom, E., Xu, N., 2020. The time variation in risk appetite and uncertainty .

Bekaert, G., Hodrick, R. J., Zhang, X., 2009. International stock return comovements. The Journal of Finance 64, 2591–2626.

Bekaert, G., Hoerova, M., 2014. The vix, the variance premium and stock market volatility. Journal of Econometrics 183, 181–192.

Bollerslev, T., Gibson, M., Zhou, H., 2011. Dynamic estimation of volatility risk premia and investor risk aversion from option-implied and realized volatilities. Journal of Econometrics 160, 235–245.

Bollerslev, T., Marrone, J., Xu, L., Zhou, H., 2014. Stock return predictability and variance risk premia: statistical inference and international evidence. Journal of Financial and Quantitative Analysis 49, 633–661.

Bollerslev, T., Tauchen, G., Zhou, H., 2009. Expected stock returns and variance risk premia. The Review of Financial Studies 22, 4463–4492.

Bollerslev, T., Zhou, H., 2006. Volatility puzzles: a simple framework for gauging return-volatility regressions. Journal of Econometrics 131, 123–150.

Brandt, M. W., Kang, Q., 2004. On the relationship between the conditional mean and volatility of stock returns: A latent var approach. Journal of Financial Economics 72, 217–257.

Britten-Jones, M., Neuberger, A., 2000. Option prices, implied price processes, and stochastic volatility. The Journal of Finance 55, 839–866.

Campbell, J. Y., Cochrane, J. H., 1999. By force of habit: A consumption-based explanation of aggregate stock market behavior. Journal of political Economy 107, 205–251.

Christoffersen, P., Errunza, V., Jacobs, K., Langlois, H., 2012. Is the potential for international diversification disappearing? a dynamic copula approach. The Review of Financial Studies 25, 3711–3751.

Colacito, R., Croce, M. M., 2010. The short and long run benefits of financial integration. American Economic Review 100, 527–31.

Corradi, V., Distaso, W., Mele, A., 2013. Macroeconomic determinants of stock market volatility and volatility risk premiums. Journal of Monetary Economics 60, 203–220.

Corsi, F., 2009. A simple approximate long-memory model of realized volatility. Journal of Financial Econometrics 7, 174–196.

David, A., Veronesi, P., 2013. What ties return volatilities to price valuations and fundamentals? Journal of Political Economy 121, 682–746.

Drechsler, I., Yaron, A., 2010. What's vol got to do with it. The Review of Financial Studies 24, 1–45.

Duffee, G. R., 2005. Time variation in the covariance between stock returns and consumption growth. The Journal of Finance 60, 1673–1712.

Ebert, S., 2015. On skewed risks in economic models and experiments. Journal of Economic Behavior & Organization 112, 85–97.

Feunou, B., Jahan-Parvar, M. R., Okou, C., 2017. Downside variance risk premium. Journal of Financial Econometrics 16, 341–383.

Ghysels, E., Santa-Clara, P., Valkanov, R., 2005. There is a risk-return trade-off after all. Journal of Financial Economics 76, 509–548.

Gourinchas, P.-O., Jeanne, O., 2006. The elusive gains from international financial integration. The Review of Economic Studies 73, 715–741.

Held, M., Kapraun, J., Omachel, M., Thimme, J., 2018. Up-and downside variance risk premia in global equity markets .

Jacquier, E., Okou, C., 2013. Disentangling continuous volatility from jumps in long-run risk–return relationships. Journal of Financial Econometrics 12, 544–583.

Jurado, K., Ludvigson, S. C., Ng, S., 2015. Measuring uncertainty. American Economic Review 105, 1177–1216.

Kilic, M., Shaliastovich, I., 2018. Good and bad variance premia and expected returns. Management Science .

Londono, J. M., 2015. The variance risk premium around the world .

Londono, J. M., Zhou, H., 2017. Variance risk premiums and the forward premium puzzle. Journal of Financial Economics 124, 415–440.

Ludvigson, S. C., Ng, S., 2007. The empirical risk–return relation: A factor analysis approach. Journal of Financial Economics 83, 171–222.

Malmendier, U., Nagel, S., 2011. Depression babies: do macroeconomic experiences affect risk taking? The Quarterly Journal of Economics 126, 373–416.

Merton, R. C., et al., 1973. An intertemporal capital asset pricing model. Econometrica 41, 867–887.

Miranda-Agrippino, S., Rey, H., 2018. World asset markets and the global financial cycle. Tech. rep., National Bureau of Economic Research.

Stiglitz, J. E., 2010. Risk and global economic architecture: Why full financial integration may be undesirable. American Economic Review 100, 388–92.

Wachter, J. A., 2006. A consumption-based model of the term structure of interest rates. Journal of Financial economics 79, 365–399.

Xu, N., 2019. Global risk aversion and international return comovements .

Xu, N. R., forthcoming. Procyclicality of the comovement between dividend growth and consumption growth. Journal of Financial Economics .

Zhou, H., 2010. Variance risk premia, asset predictability puzzles, and macroeconomic uncertainty .

Table 1: Expected downside and upside realized variances

This table shows the coefficients associated with the predictors of one-month-ahead (22 days) downside and upside realized variances, in panels A and B, respectively. The specification in column (1) assumes that realized variances follow a Martingale ($E(rv^i_{t+1}) = rv^i_t$, for $i = D, U$ (downside or upside)). For the specifications in columns (2) to (7), we estimate the following regression setting:

$$E_t(rv^i_{t+1m}) = \hat{\alpha}^i + \hat{\gamma}^{\mathbf{i}}\mathbf{X^i_t}.$$

We consider the following predictors at time t, $\mathbf{X_t}$: the total realized variance calculated over the last month ($rv_{t-1m,t}$) and its downside an upside components ($rv^i_{t-1m,t}$); realized semivariances calculated using either the last five days ($rv^i_{t-5d,t}$) or the last day of the month ($rv^i_{t-1d,t}$); and the option-implied variance ($iv_{t,t+1m}$) and its downside and upside components ($iv^i_{t,t+1m}$). All regressions are estimated using daily data. The sample runs from April 1991 to March 2018. Heteroskedasticity and autocorrelation consistent (HAC) standard deviations with 44 lags are reported in parentheses. *** (**, *) represent significance at the 1% (5%, 10%) confidence level. We also report the following two measures for the relative fit of each model: the adjusted R^2 and the Bayesian information criterion (BIC). The chosen specification has the lowest BICs among the seven specifications that we consider.

	(1)	(2)	(3)	(4)	(5)	(6)	(7)
				A. Downside VP			
							Chosen
Constant	0	4.01***	4.32***	4.07***	2.20***	3.36***	**2.75*** **
	-	(0.85)	(0.69)	(0.58)	(0.62)	(1.12)	**(0.98)**
$rv_{t-1m,t}$			0.14				
			(0.22)				
$rv^D_{t-1m,t}$	1	0.64***	0.34	0.28***	0.31***	0.20**	**0.18***
	-	(0.10)	(0.38)	(0.09)	(0.10)	(0.09)	**(0.11)**
$rv^D_{t-5d,t}$				0.32**		0.30*	**0.28***
				(0.15)		(0.17)	**(0.16)**
$rv^D_{t-1d,t}$				0.05***		0.04	**0.03**
				(0.02)		(0.03)	**(0.02)**
$iv_{t,t+1m}$							**0.37**
							(0.23)
$iv^D_{t,t+1m}$					0.22***	0.07	**-0.43**
					(0.05)	(0.11)	**(0.39)**
Adj. R^2	0.27	0.38	0.40	0.32	0.45	0.35	**0.38**
BIC	107,979.91	106,342.73	71,052.28	70,607.35	70,901.20	70,601.58	**70,542.67**
				B. Upside VP			
						Chosen	
Constant	0	3.70***	3.95***	3.51***	0.72	**1.09**	0.98
	-	(0.86)	(0.66)	(0.61)	(0.96)	**(0.76)**	(0.67)
$rv_{t-1m,t}$			0.59***				
			(0.18)				
$rv^U_{t-1m,t}$	1	0.65***	-0.56	0.31***	0.26***	**0.09**	0.06
	-	(0.10)	(0.42)	(0.09)	(0.08)	**(0.12)**	(0.11)
$rv^U_{t-5d,t}$				0.33*		**0.27**	0.27
				(0.17)		**(0.17)**	(0.17)
$rv^U_{t-1d,t}$				0.05***		**0.03****	0.03**
				(0.01)		**(0.01)**	(0.01)
$iv_{t,t+1m}$							0.05
							(0.13)
$iv^U_{t,t+1m}$					0.63***	**0.49*** **	0.37
					(0.13)	**(0.10)**	(0.34)
Adj. R^2	0.31	0.46	0.40	0.40	0.54	**0.47**	0.47
BIC	106613.762	105,052.17	69,832.93	69,521.93	69,487.41	**69,226.92**	69,229.04

Table 2: Summary statistics for variance premium components

This table reports time series averages of the monthly risk-neutral and physical expectations of the variances ("$iv_{t,t+1m}$" and "$E_t(rv_{t,t+1m})$") as well as the corresponding monthly variance premiums (VPs). The monthly time series are end-of-month estimates from Table 1. All measures are in units of monthly variance—i.e., in annual percentage squared divided by 12 (as commonly used in the literature; see e.g. Bekaert and Hoerova (2014), Kilic and Shaliastovich (2018) among many others). For VP estimates, we also report standard deviations and minimum and maximum values. The sample runs from April 1991 to March 2018.

	(1)	(2)	(3)	(4)	(5)	(6)	(7)
				A. DVP			
							Chosen
$iv^D_{t,t+1m}$	24.29	24.29	24.29	24.29	24.29	24.29	**24.29**
$E_t(rv^D_{t,t+1m})$	11.09	11.08	11.11	10.85	11.01	10.83	**10.81**
$vp^D_{t,t+1m}$	13.19	13.20	13.17	13.44	13.27	13.45	**13.48**
$SD(vp^D_{t,t+1m})$	11.52	14.29	14.70	14.46	13.57	14.16	**13.98**
$Min(vp^D_{t,t+1m})$	-20.18	-1.27	-1.57	-1.55	0.53	-0.88	**-1.28**
$Max(vp^D_{t,t+1m})$	81.25	93.28	96.81	89.34	94.40	95.21	**101.10**
				B. UVP			
						Chosen	
$iv^U_{t,t+1m}$	11.17	11.17	11.17	11.17	11.17	**11.17**	11.17
$E_t(rv^U_{t,t+1m})$	10.74	10.71	10.77	10.70	10.59	**10.59**	10.59
$vp^U_{t,t+1m}$	0.44	0.47	0.40	0.47	0.58	**0.58**	0.58
$SD(vp^U_{t,t+1m})$	10.04	6.40	6.31	6.51	2.52	**3.81**	3.75
$Min(vp^U_{t,t+1m})$	-138.25	-65.12	-67.14	-66.95	-28.53	**-40.84**	-39.90
$Max(vp^U_{t,t+1m})$	23.27	27.48	19.37	22.63	10.31	**10.28**	11.42

Table 3: Correlations

This table reports correlations among the monthly total, downside, and upside variance premiums across various measures. The first seven columns of Panel A reports correlations of VP estimates from the same model from Table 1; the last column, "chosen", reports correlations of the chosen VP measures (measure (7) for DVP and measure (6) for UVP, according to Table 1). Panel B (Panel C) reports correlations of DVP (UVP) estimates across measures. Chosen models are shown in bold. *** (**, *) represent significance at the 1% (5%, 10%) confidence level using bootstrapped standard errors (10,000 times). The sample runs from April 1991 to March 2018.

	(1)	(2)	(3)	(4)	(5)	(6)	(7)	**Chosen**
A. Correlations within models								
Correl(VP,DVP)	0.84***	0.95***	0.94***	0.93***	0.98***	0.97***	0.97***	**0.95*** **
Correl(VP,UVP)	0.79***	0.68***	0.63***	0.57***	0.31	0.29*	0.23	**0.35***
Correl(UVP,DVP)	0.33***	0.41**	0.34*	0.22	0.14	0.04	-0.03	**0.11**
B. Correlations across measures; DVP								
(1)	1.00							
(2)	0.88***	1.00						
(3)	0.87***	1.00***	1.00					
(4)	0.76***	0.96***	0.97***	1.00				
(5)	0.76***	0.98***	0.98***	0.98***	1.00			
(6)	0.74***	0.96***	0.96***	1.00***	0.98***	1.00		
(7)	**0.74*** **	**0.95*** **	**0.96*** **	**0.99*** **	**0.98*** **	**0.99*** **	**1.00**	
C. Correlations across measures; UVP								
(1)	1.00							
(2)	0.81***	1.00						
(3)	0.77***	0.94***	1.00					
(4)	0.77***	0.89***	0.87***	1.00				
(5)	0.89***	0.99***	0.93***	0.89***	1.00			
(6)	**0.76*** **	**0.77*** **	**0.76*** **	**0.97*** **	**0.79*** **	**1.00**		
(7)	0.74***	0.77***	0.78***	0.97***	0.79***	0.99***	1.00	

Table 4: The null predictive regression specification: country-level regression with total variance risk premium

This table reports the country-level univariate predictability regression coefficient estimates where the predictor is the total variance risk premium. The regression setting is the following:

$$h^{-1}r_{i,t,t+h} = a_{i,h} + b_{i,h}(vp^{D}_{t,t+1} + vp^{U}_{t,t+1}) + \epsilon_{i,t,t+h},$$

where $r_{i,t,t+h}$ denotes the cumulative h-month-ahead log excess returns for country i. The table reports the results at various horizons of interest (in units of months). The estimates and their Newey-West standard errors (in parentheses) are reported along with the adjusted R^2. *** (**, *) represent significance at the 1% (5%, 10%) confidence level.

	h=1		h=3		h=6		h=12	
Country	Est (SE)	R^2	Est (SE)	R^2	Est (SE)	R^2	Est (SE)	R^2
Australia	0.3757	0.59%	0.4792***	2.73%	0.5159***	5.76%	0.3129***	4.48%
	(0.2727)		(0.1601)		(0.1174)		(0.0821)	
Austria	-0.1748	0.09%	0.1649	0.19%	0.3282**	1.31%	0.0745	0.14%
	(0.3212)		(0.2090)		(0.1603)		(0.1130)	
Belgium	-0.2155	0.22%	0.0369	0.02%	0.0855	0.15%	-0.0312	0.04%
	(0.2542)		(0.1627)		(0.1242)		(0.0895)	
Canada	0.2216	0.23%	0.4187***	2.08%	0.458***	4.63%	0.2779***	3.59%
	(0.2552)		(0.1608)		(0.1170)		(0.0818)	
Denmark	-0.0622	0.02%	0.2416	0.73%	0.2893**	1.80%	0.1391	0.86%
	(0.2583)		(0.1576)		(0.1201)		(0.0847)	
Finland	0.3036	0.21%	0.3825*	0.86%	0.3779**	1.55%	0.1760	0.62%
	(0.3661)		(0.2295)		(0.1694)		(0.1269)	
France	-0.0019	0.00%	0.2355	0.72%	0.2808**	1.91%	0.1508*	1.09%
	(0.2679)		(0.1544)		(0.1132)		(0.0817)	
Germany	-0.0760	0.02%	0.1749	0.32%	0.2198*	0.96%	0.0609	0.15%
	(0.2970)		(0.1719)		(0.1255)		(0.0891)	
Hong Kong	0.1582	0.07%	0.2223	0.39%	0.2562*	1.09%	0.1324	0.56%
	(0.3296)		(0.1980)		(0.1375)		(0.1002)	
Ireland	-0.1292	0.07%	0.1149	0.13%	0.1402	0.31%	-0.1020	0.30%
	(0.2756)		(0.1775)		(0.1414)		(0.1054)	
Italy	0.0841	0.02%	0.2654	0.64%	0.3012**	1.48%	0.0874	0.25%
	(0.3314)		(0.1847)		(0.1383)		(0.0985)	
Japan	-0.1642	0.13%	0.1705	0.37%	0.3545***	2.85%	0.2783***	3.33%
	(0.2564)		(0.1562)		(0.1165)		(0.0852)	
Netherlands	-0.2470	0.25%	0.0765	0.07%	0.1070	0.23%	-0.0076	0.00%
	(0.2754)		(0.1653)		(0.1243)		(0.0898)	
New Zealand	-0.1484	0.09%	0.1738	0.37%	0.2926**	1.78%	0.1485	0.82%
	(0.2812)		(0.1589)		(0.1224)		(0.0928)	
Norway	0.0120	0.00%	0.2245	0.36%	0.2822*	1.03%	0.1636	0.72%
	(0.3307)		(0.2087)		(0.1554)		(0.1091)	
Portugal	-0.0044	0.00%	0.1611	0.23%	0.1188	0.22%	-0.0591	0.11%
	(0.2998)		(0.1860)		(0.1419)		(0.1024)	
Singapore	0.3085	0.31%	0.5312***	2.36%	0.571***	4.98%	0.4526***	5.90%
	(0.3106)		(0.1914)		(0.1403)		(0.1027)	
Spain	0.2528	0.20%	0.3621**	1.26%	0.2547*	1.17%	0.0110	0.00%
	(0.3133)		(0.1792)		(0.1317)		(0.0947)	
Sweden	0.3639	0.40%	0.5686***	2.78%	0.5868***	4.98%	0.379***	3.87%
	(0.3209)		(0.1884)		(0.1442)		(0.1073)	
Switzerland	-0.3776*	0.92%	-0.0581	0.06%	0.0314	0.03%	-0.0414	0.12%
	(0.2186)		(0.1294)		(0.0952)		(0.0692)	
U.K.	0.0164	0.00%	0.1916	0.69%	0.2271**	1.66%	0.1042	0.66%
	(0.2119)		(0.1285)		(0.0983)		(0.0727)	
U.S.	0.0907	0.07%	0.2292**	1.33%	0.2413***	2.57%	0.1196*	1.12%
	(0.1889)		(0.1106)		(0.0835)		(0.0638)	

Table 5: Specification (1), country-level multivariate regression results with DVP and UVP: Model comparisons against the null

This table reports the country-level multivariate predictability regression results where the predictors are downside and upside variance risk premiums. Specification (1) is the regression setting in Equation (7) (Section 3),

$$h^{-1}r_{i,t,t+h} = a_{i,h} + b_{i,h,D}vp^{D}_{t,t+1} + b_{i,h,U}vp^{U}_{t,t+1} + \epsilon_{i,t,t+h}.$$

Panel A provides AICs, Panel B BICs, and Panel C Adjusted R^2s. Bold values indicate that Specification (1) outperforms the null regression specification (see Table 4) according to each fit measure. In the last row of each panel, we calculate the percentage of countries for which Specification (1) outperforms the null regression specification. The country-level coefficient estimates for this model are shown in Figures 5 and 6 (downside and upside, respectively).

A. AIC

	h=1		h=3		h=6		h=12	
Country	AIC (Null)	AIC (S(1))	AIC (Null)	AIC (S(1))	AIC (Null)	AIC (S(1))	AIC (Null)	AIC (S(1))
Australia	3672.15	**3667.45**	3307.26	**3305.03**	3077.26	**3077.09**	2792.57	**2790.42**
Austria	3777.77	**3771.41**	3478.22	**3476.28**	3275.54	**3275.44**	2992.14	**2991.39**
Belgium	3626.78	**3619.52**	3317.33	**3315.35**	3113.26	**3112.93**	2847.00	**2846.51**
Canada	3629.13	**3620.47**	3310.05	**3305.75**	3074.92	**3073.75**	2790.50	**2790.50**
Denmark	3637.04	**3633.96**	3296.91	**3296.29**	3091.88	**3091.84**	2812.40	**2811.63**
Finland	3862.27	**3858.11**	3538.25	**3536.31**	3310.48	**3310.28**	3064.77	**3064.70**
France	3660.65	**3657.00**	3283.91	**3279.51**	3054.04	**3052.47**	2789.73	**2789.73**
Germany	3727.08	**3724.53**	3352.65	**3350.56**	3119.99	**3119.39**	2843.82	**2843.63**
Hong Kong	3794.42	**3794.27**	3443.58	**3443.57**	3177.94	**3177.84**	2917.10	**2915.54**
Ireland	3678.90	**3670.86**	3373.31	**3369.42**	3195.54	**3195.23**	2948.74	**2948.66**
Italy	3797.95	**3795.62**	3398.86	**3395.57**	3181.75	**3179.73**	2906.75	**2906.74**
Japan	3632.14	**3630.85**	3291.32	**3290.48**	3072.44	**3072.30**	2815.74	**2814.25**
Netherlands	3678.35	**3676.96**	3327.68	**3326.67**	3113.82	**3113.08**	2848.90	**2848.61**
New Zealand	3691.99	**3690.14**	3302.21	**3301.14**	3103.84	**3103.84**	2869.62	**2866.96**
Norway	3796.71	**3787.75**	3477.40	**3475.41**	3255.53	**3255.39**	2970.14	**2969.84**
Portugal	3733.15	**3731.74**	3403.51	**3401.97**	3197.92	**3197.72**	2930.99	**2930.67**
Singapore	3756.08	**3754.65**	3421.65	**3421.32**	3190.57	**3190.48**	2932.47	**2930.76**
Spain	3761.78	**3760.55**	3379.39	**3376.98**	3150.27	**3148.51**	2881.81	**2881.45**
Sweden	3777.17	**3775.67**	3411.66	**3410.80**	3208.09	**3208.04**	2960.16	**2959.07**
Switzerland	3529.31	**3527.04**	3170.67	**3167.14**	2944.31	**2941.30**	2686.02	**2686.02**
U.K.	3509.23	**3503.23**	3166.09	**3160.29**	2964.28	**2961.79**	2716.60	**2716.60**
U.S.	3434.83	**3428.25**	3069.66	**3062.49**	2860.82	**2858.62**	2635.25	**2635.25**
% of S(1) Outperforms	100%		100%		100%		100%	

B. BIC

	h=1		h=3		h=6		h=12	
Country	BIC (Null)	BIC (S(1))	BIC (Null)	BIC (S(1))	BIC (Null)	BIC (S(1))	BIC (Null)	BIC (S(1))
Australia	3679.71	**3675.00**	3314.80	**3312.57**	3084.78	**3084.62**	2800.06	**2797.90**
Austria	3785.32	**3778.97**	3485.76	**3483.82**	3283.06	**3282.96**	2999.62	**2998.88**
Belgium	3634.33	**3627.07**	3324.87	**3322.89**	3120.79	**3120.45**	2854.49	**2854.00**
Canada	3636.69	**3628.02**	3317.59	**3313.30**	3082.45	**3081.28**	2797.99	**2797.99**
Denmark	3644.60	**3641.52**	3304.45	**3303.84**	3099.40	**3099.36**	2819.88	**2819.12**
Finland	3869.83	**3865.67**	3545.79	**3543.85**	3318.00	**3317.80**	3072.25	**3072.19**
France	3668.21	**3664.55**	3291.45	**3287.06**	3061.56	**3059.99**	2797.22	**2797.21**
Germany	3734.64	**3732.09**	3360.20	**3358.11**	3127.52	**3126.91**	2851.31	**2851.11**
Hong Kong	3801.98	**3801.82**	3451.12	**3451.12**	3185.46	**3185.36**	2924.59	**2923.03**
Ireland	3686.46	**3678.41**	3380.86	**3376.97**	3203.06	**3202.76**	2956.22	**2956.15**
Italy	3805.51	**3803.18**	3406.40	**3403.12**	3189.27	**3187.25**	2914.23	**2914.23**
Japan	3639.69	**3638.40**	3298.86	**3298.02**	3079.96	**3079.83**	2823.23	**2821.74**
Netherlands	3685.90	**3684.51**	3335.22	**3334.21**	3121.35	**3120.60**	2856.38	**2856.10**
New Zealand	3699.54	**3697.70**	3309.76	**3308.68**	3111.37	**3111.37**	2877.10	**2874.44**
Norway	3804.27	**3795.31**	3484.94	**3482.96**	3263.06	**3262.91**	2977.63	**2977.32**
Portugal	3740.71	**3739.29**	3411.05	**3409.51**	3205.44	**3205.24**	2938.48	**2938.16**
Singapore	3763.63	**3762.20**	3429.20	**3428.86**	3198.10	**3198.00**	2939.96	**2938.25**
Spain	3769.33	**3768.11**	3386.94	**3384.52**	3157.80	**3156.03**	2889.29	**2888.94**
Sweden	3784.72	**3783.23**	3419.20	**3418.35**	3215.61	**3215.56**	2967.65	**2966.56**
Switzerland	3536.87	**3534.59**	3178.21	**3174.68**	2951.83	**2948.82**	2693.51	**2693.50**
U.K.	3516.78	**3510.78**	3173.64	**3167.84**	2971.80	**2969.32**	2724.08	**2724.08**
U.S.	3442.38	**3435.80**	3077.20	**3070.03**	2868.34	**2866.14**	2642.74	**2642.73**
% of S(1) Outperforms	100%		100%		100%		100%	

(next page)

(table continues)

C. Adjusted R^2								
	h=1		h=3		h=6		h=12	
Country	R^2 (Null)	R^2 (S(1))	R^2 (Null)	R^2 (S(1))	R^2 (Null)	R^2 (S(1))	R^2 (Null)	R^2 (S(1))
Australia	0.59%	**2.03%**	2.73%	**3.40%**	5.76%	**5.81%**	4.48%	**5.14%**
Austria	0.09%	**2.04%**	0.19%	**0.80%**	1.31%	**1.34%**	0.14%	**0.38%**
Belgium	0.22%	**2.44%**	0.02%	**0.63%**	0.15%	**0.25%**	0.04%	**0.20%**
Canada	0.23%	**2.88%**	2.08%	**3.38%**	4.63%	**4.98%**	3.59%	**3.59%**
Denmark	0.02%	**0.97%**	0.73%	**0.92%**	1.80%	**1.81%**	0.86%	**1.11%**
Finland	0.21%	**1.49%**	0.86%	**1.46%**	1.55%	**1.61%**	0.62%	**0.64%**
France	0.00%	**1.12%**	0.72%	**2.07%**	1.91%	**2.39%**	1.09%	**1.09%**
Germany	0.02%	**0.81%**	0.32%	**0.97%**	0.96%	**1.15%**	0.15%	**0.21%**
Hong Kong	0.07%	**0.12%**	0.39%	**0.39%**	1.09%	**1.12%**	0.56%	**1.06%**
Ireland	0.07%	**2.53%**	0.13%	**1.33%**	0.31%	**0.41%**	0.30%	**0.33%**
Italy	0.02%	**0.74%**	0.64%	**1.65%**	1.48%	**2.10%**	0.25%	**0.25%**
Japan	0.13%	**0.53%**	0.37%	**0.63%**	2.85%	**2.89%**	3.33%	**3.79%**
Netherlands	0.25%	**0.68%**	0.07%	**0.38%**	0.23%	**0.47%**	0.00%	**0.09%**
New Zealand	0.09%	**0.66%**	0.37%	**0.71%**	1.78%	**1.78%**	0.82%	**1.66%**
Norway	0.00%	**2.74%**	0.36%	**0.97%**	1.03%	**1.08%**	0.72%	**0.82%**
Portugal	0.00%	**0.44%**	0.23%	**0.71%**	0.22%	**0.28%**	0.11%	**0.21%**
Singapore	0.31%	**0.75%**	2.36%	**2.46%**	4.98%	**5.01%**	5.90%	**6.41%**
Spain	0.20%	**0.58%**	1.26%	**2.00%**	1.17%	**1.72%**	0.00%	**0.12%**
Sweden	0.40%	**0.86%**	2.78%	**3.03%**	4.98%	**4.99%**	3.87%	**4.20%**
Switzerland	0.92%	**1.62%**	0.06%	**1.16%**	0.03%	**0.97%**	0.12%	**0.12%**
U.K.	0.00%	**1.84%**	0.69%	**2.47%**	1.66%	**2.43%**	0.66%	**0.66%**
U.S.	0.07%	**2.09%**	1.33%	**3.51%**	2.57%	**3.25%**	1.12%	**1.12%**
% of S(1) Outperforms	100%		100%		100%		100%	

Table 6: Specification (2), pooled multivariate regression results with DVP and UVP: Estimated coefficients, variance decomposition, and explanatory power

This table reports the pooled multivariate predictability regression results where the predictors are downside and upside variance risk premiums. The table provides coefficient estimates and their panel-data Newey-West autocorrelation consistent standard errors, in parentheses, at various horizons (in unit of months). We also report the adjusted R^2 and the proportion of the R^2 explained by each predictor (VARC). *** (**, *) represent significance at the 1% (5%, 10%) confidence level.

Horizon	Coef(vp^D)	NW SE	VARC(vp^D)	Coef(vp^U)	NW SE	VARC(vp^U)	R^2
1	-0.1055	(0.0720)	4%	1.7893***	(0.2081)	96%	0.88%
2	0.147**	(0.0630)	28%	0.8646***	(0.1726)	72%	0.50%
3	0.1828***	(0.0588)	29%	1.0602***	(0.1598)	71%	1.12%
4	0.1886***	(0.0570)	25%	1.1948***	(0.1644)	75%	1.74%
5	0.2303***	(0.0539)	49%	0.8526***	(0.1293)	51%	1.57%
6	0.2676***	(0.0524)	76%	0.5509***	(0.1025)	24%	1.61%
7	0.2621***	(0.0520)	93%	0.2705***	(0.0994)	7%	1.45%
8	0.2072***	(0.0524)	91%	0.2416**	(0.0980)	9%	1.05%
9	0.1837***	(0.0499)	100%	0.0115	(0.0950)	0%	0.84%
10	0.1588***	(0.0471)	99%	-0.0594	(0.0905)	1%	0.70%
11	0.1526***	(0.0432)	97%	-0.1051	(0.0880)	3%	0.73%
12	0.144***	(0.0396)	98%	-0.0809	(0.0821)	2%	0.71%

Table 7: Pooled multivariate regression results with DVP, UVP, and other predictors: Estimated coefficients, variance decomposition, and explanatory power

This table reports the pooled multivariate predictability regression results where the predictors are the following: DVP, UVP, term spread ("tsprd," calculated as the U.S. 10-year yield minus the 3-month yield; source: FRED), and dividend yield ("DY," the dividend yield of the U.S. S&P 500 stock market index; source: DataStream). The model is a special case of Equation (8) (Section 3),

$$h^{-1}r_{i,t,t+h} = a_h + b_{h,D}vp^D_{t,t+1} + b_{h,U}vp^U_{t,t+1} + c_{h,tsprd}tsprd_t + c_{h,DY}DY_t + \epsilon_{i,t,t+h}.$$

For each predictor, the first column presents the coefficient estimates and their significance level using the Newey-West standard errors reported in the second column in parentheses. The third column reports the variance decomposition (VARC), $\widehat{b_x}\frac{cov(Fitted,x)}{var(Fitted)}$, where x is any of the predictors. By design, all VARCs add up to 1. Column "R^2" reports the adjusted R^2 of the model. The table also reports an F test testing whether control predictors offer additional contribution to the null model (specification (2) in Table 6). *** (**, *) represent significance at the 1% (5%, 10%) confidence level.

Horizon	Coef(vp^D)	NW SE	VARC(vp^D)	Coef(vp^U)	NW SE	VARC(vp^U)				
1	-0.0557	(0.0089)	1%	2.0232***	(0.0208)	57%				
2	0.2016***	(0.0069)	10%	1.0899***	(0.0099)	23%				
3	0.2372***	(0.0053)	12%	1.2927***	(0.0077)	29%				
4	0.2426***	(0.0051)	12%	1.4402***	(0.0069)	33%				
5	0.2802***	(0.0049)	19%	1.0987***	(0.0069)	20%				
6	0.3138***	(0.0043)	26%	0.795***	(0.0074)	10%				
7	0.3045***	(0.0041)	29%	0.5057***	(0.0060)	4%				
8	0.2431***	(0.0042)	22%	0.4731***	(0.0063)	4%				
9	0.2131***	(0.0038)	20%	0.2342***	(0.0062)	0%				
10	0.1818***	(0.0035)	16%	0.1579*	(0.0064)	0%				
11	0.17***	(0.0032)	16%	0.1067	(0.0059)	-1%				
12	0.156***	(0.0031)	14%	0.1287*	(0.0059)	-1%				
Horizon	Coef(tsprd)	NW SE	VARC(tsprd)	Coef(DY)	NW SE	VARC(DY)	VARC(vp^D+vp^U)	R^2	F (H0:S(2))	p-value
1	-4.1804***	(0.0032)	8%	66.654***	(0.854)	33%	58%	1.65%	56.17	0%
2	-4.692***	(0.0024)	14%	66.4107***	(0.831)	53%	33%	1.98%	107.01	0%
3	-4.6515***	(0.0019)	11%	67.9058***	(0.795)	47%	41%	3.38%	165.14	0%
4	-4.5658***	(0.0018)	9%	70.5776***	(0.775)	47%	44%	4.80%	226.18	0%
5	-4.159***	(0.0016)	5%	69.4541***	(0.758)	56%	39%	5.07%	258.32	0%
6	-3.7997***	(0.0014)	2%	67.8702***	(0.739)	61%	36%	5.47%	285.34	0%
7	-3.464***	(0.0012)	1%	64.8069***	(0.714)	67%	32%	5.47%	296.01	0%
8	-2.8051***	(0.0012)	-3%	61.8148***	(0.686)	77%	25%	5.20%	303.63	0%
9	-2.1529***	(0.0011)	-6%	57.6357***	(0.668)	86%	20%	4.93%	297.71	0%
10	-1.5013**	(0.0011)	-7%	54.1682***	(0.649)	91%	16%	4.85%	300.96	0%
11	-0.9088	(0.0010)	-6%	50.8702***	(0.635)	91%	15%	4.99%	308.55	0%
12	-0.3350	(0.0010)	-3%	48.3424***	(0.627)	89%	14%	5.30%	332.88	0%

Table 8: Variance risk premium components, moment matching

This table presents the moment matching results for the Generalized Method of Moments (GMM). The GMM system estimates the loadings of downside and upside variance premiums on the four global premium state variables as implied in the theoretical model. The GMM system has 90 moments and 16 unknowns and is estimated using iterative GMM. More details are shown in Section 4.4.2. *** indicates that the model estimate is within the 90% confidence interval of the empirical point estimate in the same row.

Panel A. Moment Matching				
	Moment	Empirical	Boot. SE	Model
1	vp^D	13.471	(0.747)	13.65***
2	vp^U	0.568	(0.214)	0.574***
3	$(vp^D - E(vp^D))^2$	194.360	(37.047)	195.184***
4	$(vp^U - E(vp^U))^2$	14.496	(5.723)	14.541***
5	$(vp^D - E(vp^D))^3/(SD(vp^D)^3)$	2.683	(1.010)	2.61***
6	$(vp^U - E(vp^U))^3/(SD(vp^U)^3)$	-4.782	(4.110)	-4.319***
7	$(vp^D - E(vp^D))^4/(SD(vp^D)^4)$	12.821	(5.734)	12.849***
8	$(vp^U - E(vp^U))^4/(SD(vp^U)^4)$	50.316	(43.864)	50.057***
9	$(vp^D - E(vp^D)) * (vp^U - E(vp^U))$	0.130	(12.160)	0.469***
10	$vp^D/(vp^D + vp^U)$	1.019	(0.047)	1.022***
Panel B. Overidentification Test				
GMM J Statistics: 53.44				
Hansen's J test p-value: 0.965 (Over-identifying restrictions are valid)				

Table 9: Economic determinants of variance risk premium components

Panel A of tshis table presents the loading estimates of DVP and UVP on the four U.S. premium state variables given the following system:

$$\widehat{vp_t^D} = w_{\theta p,t}^D \widehat{\theta p}_t + w_{\theta n,t}^D \widehat{\theta n}_t + w_{qp,t}^D \widehat{qp}_t + w_{qn,t}^D \widehat{qn}_t,$$
$$\widehat{vp_t^U} = w_{\theta p,t}^U \widehat{\theta p}_t + w_{\theta n,t}^U \widehat{\theta n}_t + w_{qp,t}^U \widehat{qp}_t + w_{qn,t}^U \widehat{qn}_t,$$

where $\forall x \in \{\theta p, \theta n, qp, qn\}$,

$$w_{x,t}^D = w_{x,0}^D + w_{x,1}^D z_t,$$
$$w_{x,t}^U = w_{x,0}^U + w_{x,1}^U z_t,$$

and z_t is approximated as the current squared innovation to real economic growth. Standard errors are shown in parentheses and variance decomposition results are shown in the third row ("VARC"). Panel B presents the marginal changes in DVP or UVP given 1 SD increase in each determinant. Specifically, Panel B calculate loadings at various levels of current uncertainty realizations z_t (sample average, 90th, and 95th percentiles) using the coefficient estimates in Panel A; for the purpose of interpretation, the loadings are then multiplied by the standard deviation of the state variable.

A. Estimation results					
		θp_t	θn_t	qp_t	qn_t
DVP	Constant, w_0	-0.226***	1.257***	0.502***	0.168***
	SE	(0.004)	(0.012)	(0.003)	(0.003)
	VARC	14.87%	33.63%	39.97%	-0.89%
	Time-varying, w_1	109.414	-8622.124***	159.673***	33.529
	SE	(128.197)	(98.369)	(61.178)	(93.603)
	VARC	17.93%	-14.56%	1.40%	7.66%
UVP	Constant, w_0	0.005*	0.089***	-0.037***	-0.002
		(0.003)	(0.006)	(0.001)	(0.002)
		0.06%	-6.23%	2.37%	-0.01%
	Time-varying, w_1	-561.812***	-9009.524***	2870.665***	364.519***
		(28.314)	(34.107)	(12.830)	(20.702)
		-81.10%	106.16%	4.78%	73.98%
B. Economic magnitudes of loadings at various z_t values					
	z_t values	$\theta p_t / SD(\theta p_t)$	$\theta n_t / SD(\theta n_t)$	$qp_t / SD(qp_t)$	$qn_t / SD(qn_t)$
DVP	Mean(z_t)	-4.3395	5.9953	8.5446	0.8143
	90th(z_t)	-4.2625	3.9625	8.6409	0.8201
	95th(z_t)	-4.1278	0.4083	8.8093	0.8302
UVP	Mean(z_t)	-0.3395	-1.7736	1.2947	0.0623
	90th(z_t)	-0.7350	-3.8977	3.0260	0.1253
	95th(z_t)	-1.4266	-7.6117	6.0530	0.2355

Table 10: U.S. predictive coefficients, moment matching

This table provides moment matches of model-implied and empirical predictive coefficients of variance risk premium components and (annualized) equity risk premiums at various horizons. Our model suggests that international equity risk premiums can be written as a linear combination of real uncertainty and risk aversion state variables only ($\widehat{\theta p}_t$, $\widehat{\theta n}_t$, $\widehat{qp}_t$, and $\widehat{qn}_t$; see Tables B1 and B2) and thus can be exactly identified in the system. See estimation details in Section 4.4.3. *** indicates that the model estimate is within the 90% confidence interval of the empirical point estimate in the same row.

	$b_{US,h,D}$			$b_{US,h,U}$			$ERP_{US,h}$		
Horizon	Empirical	SE	Model	Empirical	SE	Model	Empirical	SE	Model
1	-0.0414	(0.1942)	-0.0864***	1.8530	(0.7119)	1.9058***	9.3108	(2.7320)	9.3108***
2	0.1270	(0.1406)	0.1528***	1.1123	(0.5153)	1.0129***	9.3090	(1.9763)	9.3091***
3	0.1485	(0.1136)	0.1774***	1.3055	(0.4164)	1.2383***	9.4330	(1.6141)	9.433***
4	0.1513	(0.1000)	0.182***	1.3367	(0.3661)	1.3916***	9.4152	(1.4301)	9.4152***
5	0.1771	(0.0920)	0.2268***	1.0113	(0.3368)	1.0139***	9.3903	(1.3122)	9.3903***
6	0.2075	(0.0864)	0.2616***	0.6927	(0.3162)	0.6973***	9.3751	(1.2294)	9.3748***
7	0.1918	(0.0810)	0.2515***	0.5431	(0.2960)	0.4132***	9.3529	(1.1497)	9.3529***
8	0.1568	(0.0769)	0.2019***	0.4251	(0.2810)	0.362***	9.3534	(1.0886)	9.3534***
9	0.1448	(0.0739)	0.1817***	0.2212	(0.2698)	0.1084***	9.3132	(1.0434)	9.3131***
10	0.1332	(0.0710)	0.1588***	0.1613	(0.2591)	0.0296***	9.2862	(1.0027)	9.2861***
11	0.1272	(0.0683)	0.1504***	0.1125	(0.2494)	-0.0329***	9.2627	(0.9660)	9.2627***
12	0.1209	(0.0662)	0.1404***	0.1020	(0.2414)	-0.0052***	9.2498	(0.9357)	9.2498***

Table 11: Cross-country average predictive coefficients, moment matching

This table continues Table 10 and provides moment matches of average model-implied and empirical predictive coefficients of variance risk premium components at various horizons across countries.

	Mean of $b_{i,h,D}$			Mean of $b_{i,h,U}$		
Horizon	Empirical	SE	Model	Empirical	SE	Model
1	-0.1055	(0.0463)	-0.1183***	1.7893	(0.2162)	1.748***
2	0.1470	(0.0397)	0.1311***	0.8646	(0.1564)	0.8389***
3	0.1828	(0.0341)	0.1687***	1.0602	(0.0988)	1.0506***
4	0.1886	(0.0330)	0.1746***	1.1948	(0.0887)	1.1879***
5	0.2303	(0.0336)	0.2152***	0.8526	(0.0691)	0.852***
6	0.2676	(0.0340)	0.2539***	0.5509	(0.0512)	0.5637***
7	0.2621	(0.0333)	0.2511***	0.2705	(0.0454)	0.2931***
8	0.2072	(0.0324)	0.2004***	0.2416	(0.0465)	0.2521***
9	0.1837	(0.0321)	0.1789***	0.0115	(0.0390)	0.0253***
10	0.1588	(0.0324)	0.1557***	-0.0594	(0.0415)	-0.0429***
11	0.1526	(0.0323)	0.1503***	-0.1051	(0.0422)	-0.0885***
12	0.1440	(0.0321)	0.1418***	-0.0809	(0.0390)	-0.0698***

Table 12: Relative changes in predictive coefficients when deleting one channel: an average country

This table demonstrates the relative contributions of the four premium state variables in explaining the positive predictive coefficients of downside and upside variance premiums of an average country (i.e., $\boldsymbol{x^i} = 0$) at various horizons. "Deleting" one channel is done by: (1) setting the v loadings associated with the state variable to be 0; (2) obtaining $\widetilde{\widehat{b_{h,D}}}$ using Equation (36); (3) calculating the relative change $= \frac{\widetilde{\widehat{b_{h,D}}} - \widehat{b_{h,D}}}{\widehat{b_{h,D}}}$. The sum of the four numbers in the same row is -1 by design. The more negative the changes are, the more positive contributions the state variable carries; negative values are marked in bold. Same procedure is conducted for the UVP predictive coefficients.

	Δ DVP Predictability				Δ UVP Predictability			
Horizon	θp	θn	qp	qn	θp	θn	qp	qn
1	2.40	**-6.66**	4.29	**-1.04**	0.02	**-1.18**	0.23	**-0.07**
2	**-0.27**	3.78	**-4.96**	0.45	0.00	**-1.54**	0.62	**-0.08**
3	**-1.82**	3.16	**-2.89**	0.56	0.04	**-1.32**	0.37	**-0.09**
4	0.06	4.07	**-5.87**	0.73	**-0.01**	**-1.56**	0.69	**-0.12**
5	1.27	3.01	**-5.48**	0.21	**-0.06**	**-1.98**	1.10	**-0.06**
6	0.77	1.93	**-3.61**	**-0.09**	**-0.06**	**-2.27**	1.29	0.03
7	**-0.33**	0.87	**-1.90**	0.36	0.01	**-1.95**	1.30	**-0.35**
8	**-0.89**	0.77	**-1.14**	0.26	0.11	**-1.61**	0.72	**-0.22**
9	**-1.17**	0.01	**-0.58**	0.74	1.38	**-0.22**	3.27	**-5.43**
10	**-0.77**	**-0.07**	**-0.56**	0.41	**-0.41**	**-0.70**	**-1.62**	1.73
11	**-0.52**	**-0.11**	**-0.55**	0.18	**-0.13**	**-0.48**	**-0.74**	0.35
12	**-0.68**	**-0.20**	**-0.57**	0.45	**-0.18**	**-1.08**	**-0.92**	1.18
Mean [2,7]	**-0.05**	2.80	**-4.12**	0.37	**-0.01**	**-1.77**	0.89	**-0.11**

Table 13: Relative economic importance of real and financial integration in international stock return predictability

This table demonstrates the relative contribution of the four variance premium state variables on international stock return predictability for countries with different levels of market integration. We consider two integration channels: the real channel, which is proxied by the standardized level of the trade-to-GDP ratio, and the financial channel, which is proxied by the standardized level of the credit-to-GDP ratio. An average country has a combination of (trade-to-GDP, credit-to-GDP) of (0,0), as shown in Table 12. The combination (1,0) ((-1,0)) indicates a country with a trade-to-GDP value that is 1 SD above (below) the average and an average credit-to-GDP value, and (0,1) ((0,-1)) a country with a credit-to-GDP ratio that is 1 SD above (below) average and an average trade-to-GDP value. This table reports average changes in the predictability after deleting one channel over horizons between two and seven months when both predictive coefficients of DVP and UVP are significant for most countries. Row (0,0) is obtained from the last row of Table 12, summarizing the results for an average country; the bottom two panels report the results for a more and a less integrated country; Tables v and vi of the internet appendix provide detailed tables to generate the numbers reported in this table. * indicates that this value has the larger absolute difference from (0,0) in the same column-panel; bold columns indicate the premium state variable with the highest explanatory for (0,0) according to Table 12.

	Δ DVP predictability				Δ UVP predictability			
(Trade-to-GDP, credit-to-GDP)	θp	θn	$\boldsymbol{qp}$	qn	θp	$\boldsymbol{\theta n}$	qp	qn
(0,0)	-0.05	2.80	**-4.12**	0.37	-0.01	**-1.77**	0.89	-0.11
A more integrated country:								
(1,0)	1.84	2.84	**-6.06**	0.39	-0.22	**-3.06***	2.46	-0.18
(0,1)	5.95	5.97	**-13.78***	0.86	-0.15	**-2.48**	1.79	-0.15
A less integrated country:								
(-1,0)	-2.84	2.76	**-1.27**	0.35	0.11	**-1.00***	-0.05	-0.07
(0,-1)	-2.41	1.64	**-0.42***	0.18	0.09	**-1.29**	0.29	-0.08

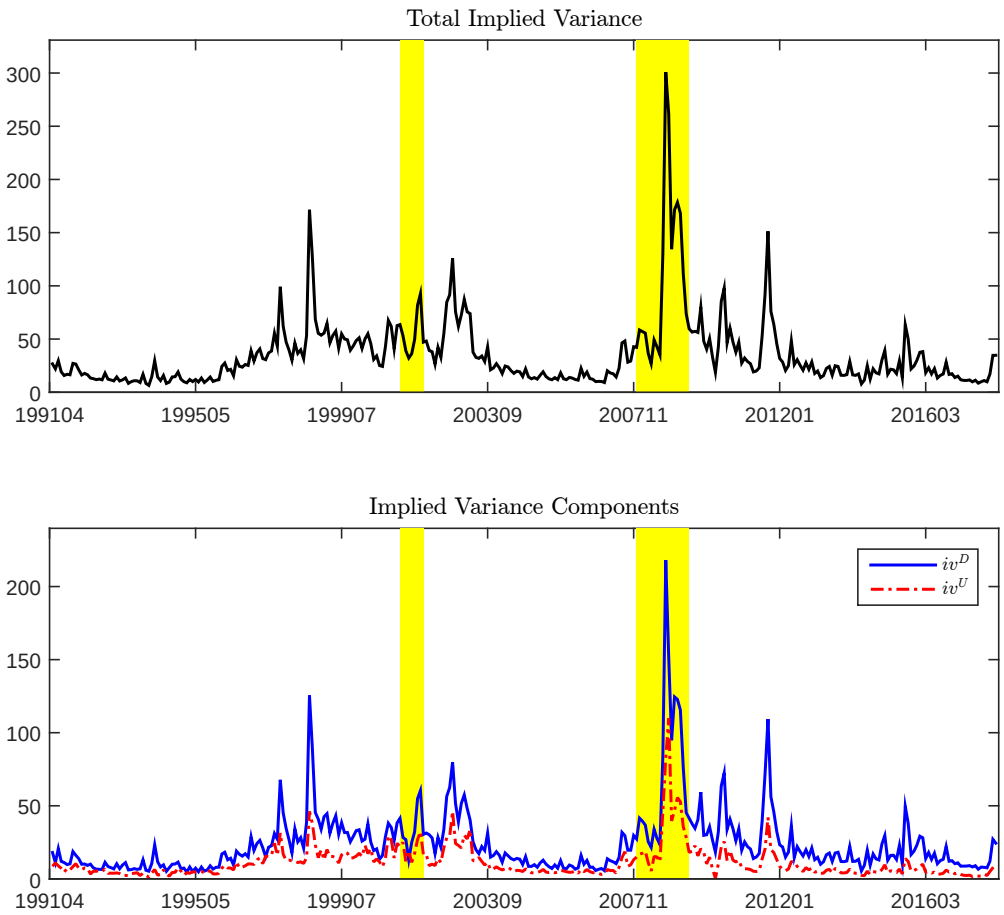

Figure 1: Option-implied variance and its downside and upside components

This figure shows the time series of total option-implied variance (top panel) and its downside and upside components (bottom panel). The construction details for option-implied variances are discussed in Section 2. Measures are in units of monthly percentages (i.e., in the same unit as VIX-squared divided by 12, or annual percentage squared divided by 12).

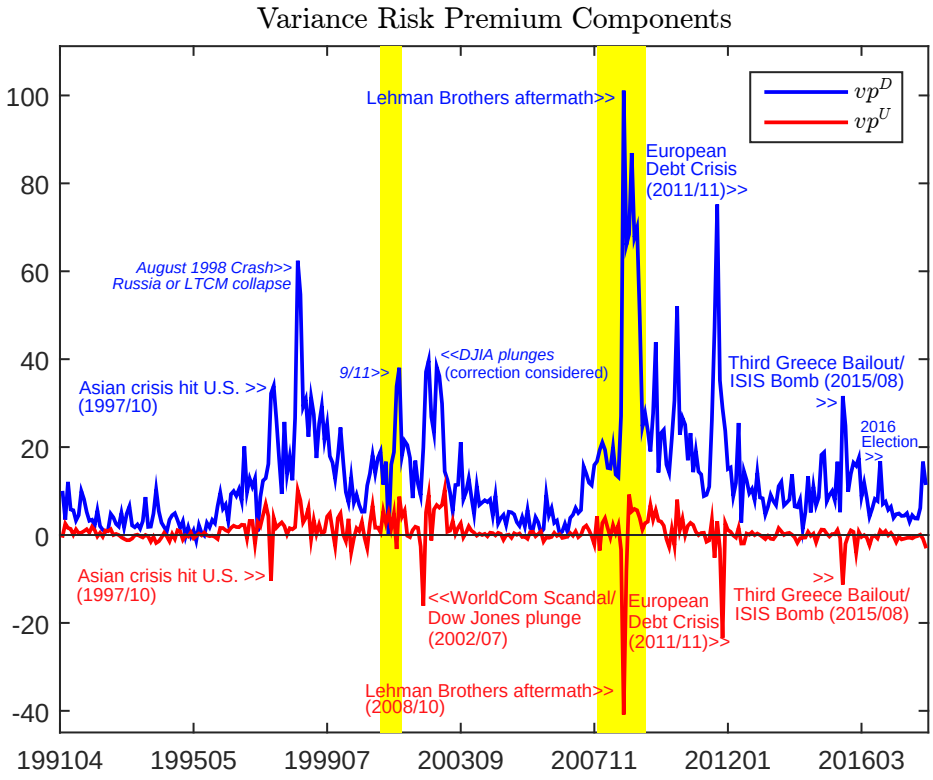

Figure 2: Downside and upside components of the variance risk premium

This figure shows the time series of the downside and upside variance premium components. The construction details of variance risk premiums are discussed in Section 2. The downside (upside) variance risk premium is calculated as the difference between the option-implied downside (upside) variance and the expected downside (upside) realized variance. We use the "chosen" forecasts of the downside and upside realized variances from Table 1. Measures are in units of monthly percentages. Total variance premium and alternative measures are available in the internet appendix.

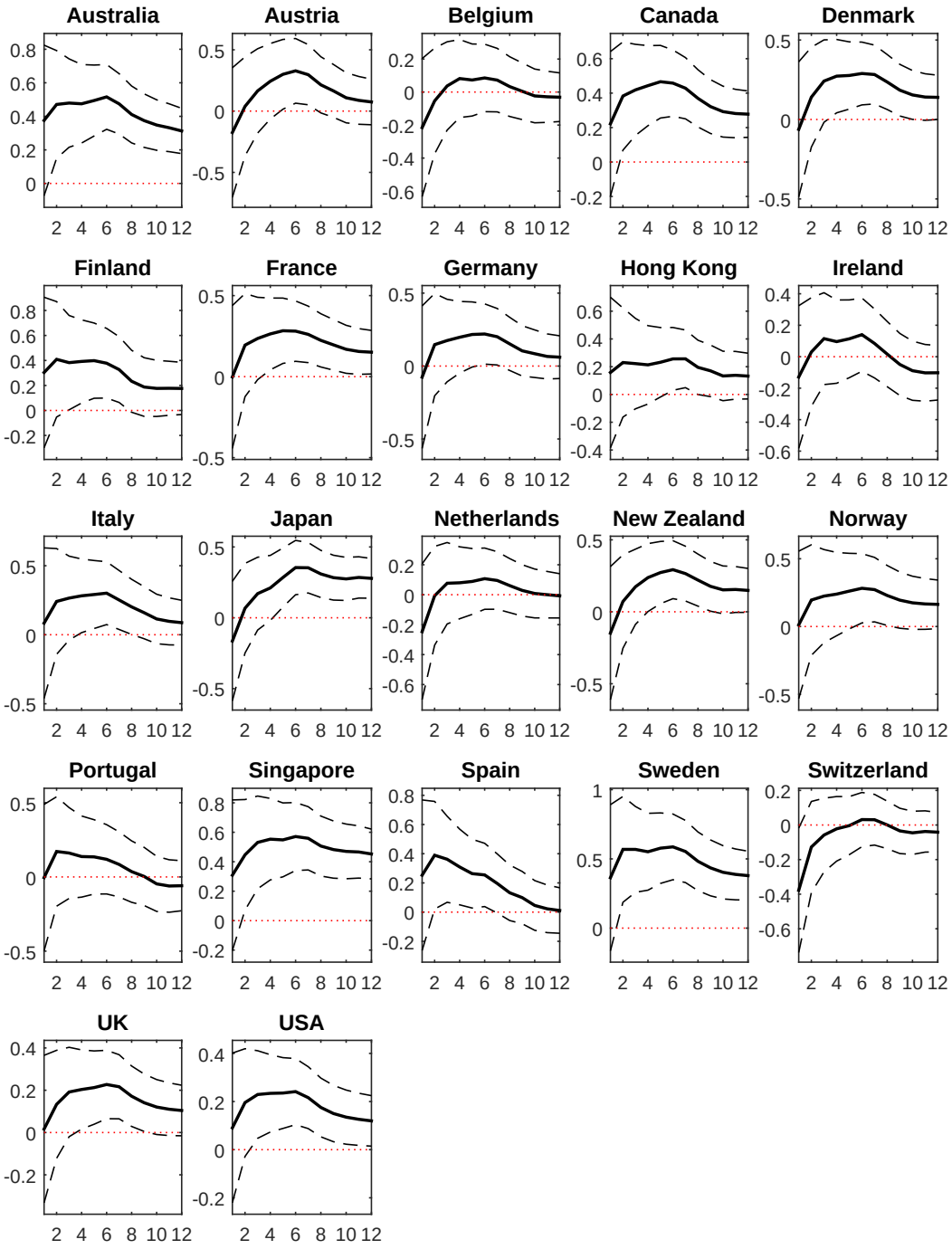

Figure 3: Total VP coefficients, null regression specification

This figure shows the predictive coefficient estimates of the total VP (the solid lines) and its 90% confidence interval given NW standard errors (the dashed lines) at the country level. The regression setting is the following:

$$h^{-1} r_{i,t,t+h} = a_{i,h} + b_{i,h}(vp^{D}_{t,t+1} + vp^{U}_{t,t+1}) + \epsilon_{i,t,t+h},$$

where $r_{i,t,t+h}$ denotes the cumulative h-month-ahead log excess returns for country i. The table corresponding to this plot is Table 4.

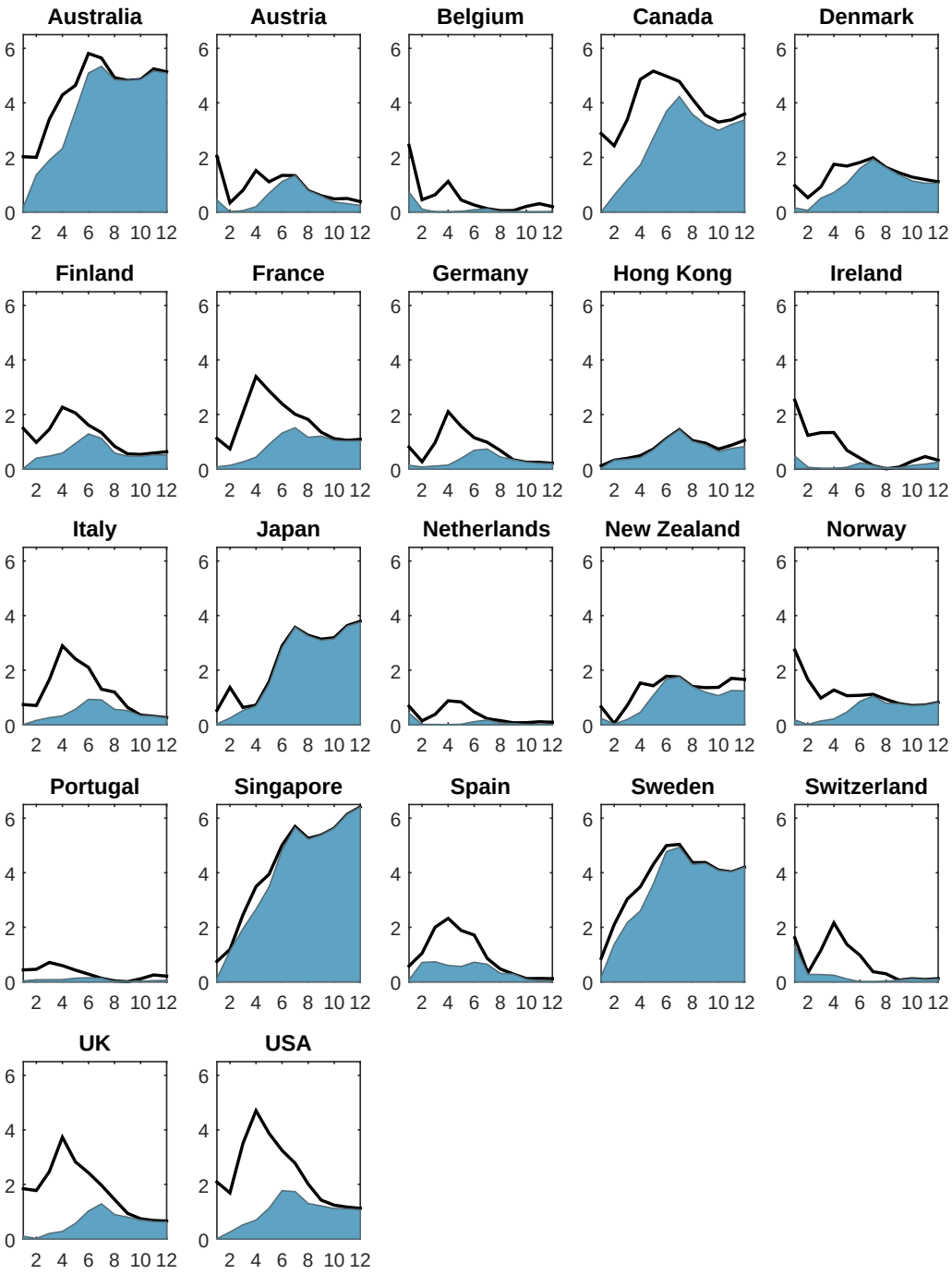

Figure 4: Explanatory power of DVP and UVP, specification (1)

The figure shows the portion of the total R^2 explained by DVP and UVP in the country-specific regression specification (specification (1)). The solid line represents the total adjusted R^2 at the country level. The blue region represents the part that is explained by DVP and the remaining area denotes the total variance explained by UVP. The table corresponding to this plot is Table 5.

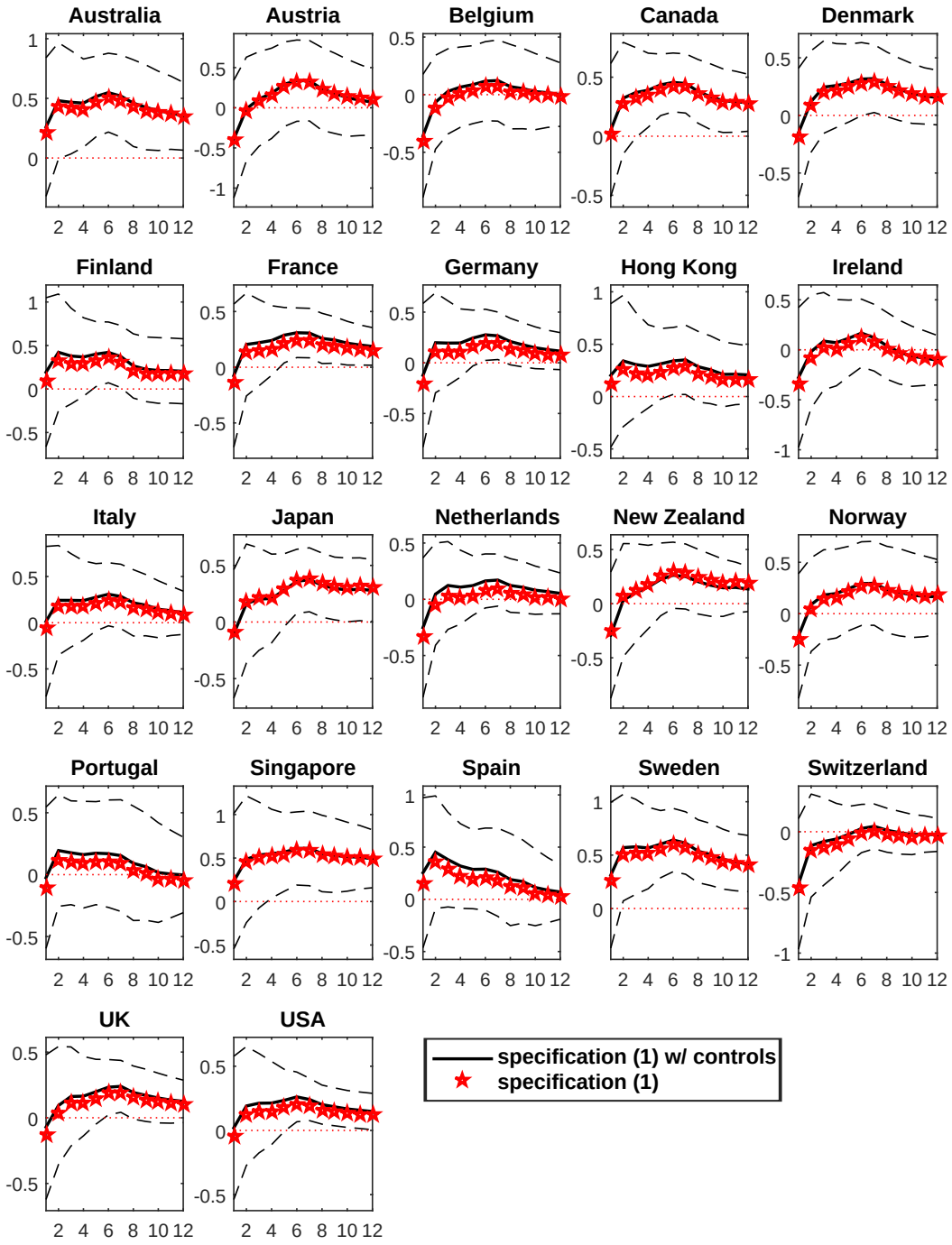

Figure 5: DVP predictive coefficients, compare model with control predictors

This figure shows the predictive coefficient estimates of DVP from the country-level predictive regression specification (1), where DVP and UVP are the predictors (the red stars), and a model where DVP, UVP, the term spread, and the dividend yield are the predictors (the solid lines). The dashed lines correspond to the 90% confidence intervals for the latter model's estimates given NW standard errors; the confidence intervals for specification (1) estimates are statistically indifferent and are hence omitted for illustration purpose. The tables corresponding to this plot are Table 5 and Table iv of the Internet Appendix. The model specification is introduced in Section 3.

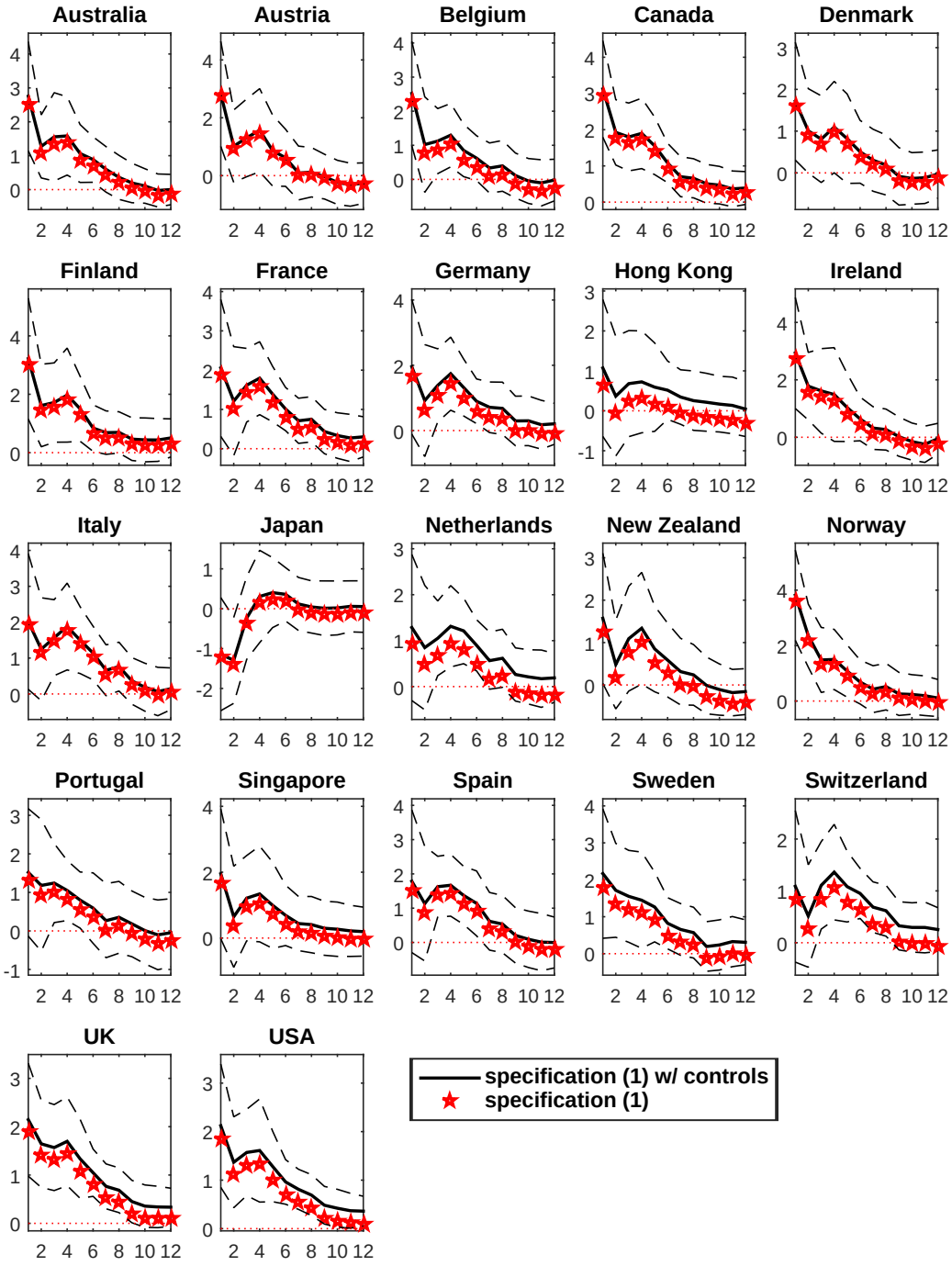

Figure 6: UVP predictive coefficients, compare model with control predictors

This figure shows the predictive coefficient estimates of UVP from the country-level predictive regression specification (1), where DVP and UVP are the predictors (the red stars), and a model where DVP, UVP, the term spread, and the dividend yield are the predictors (the solid lines). The dashed lines correspond to the 90% confidence intervals for the latter model's estimates given NW standard errors; the confidence intervals for specification (1) estimates are statistically indifferent and are hence omitted for illustration purpose. The tables corresponding to this plot are Table 5 and Table iv of the Internet Appendix. The model specification is introduced in Section 3.

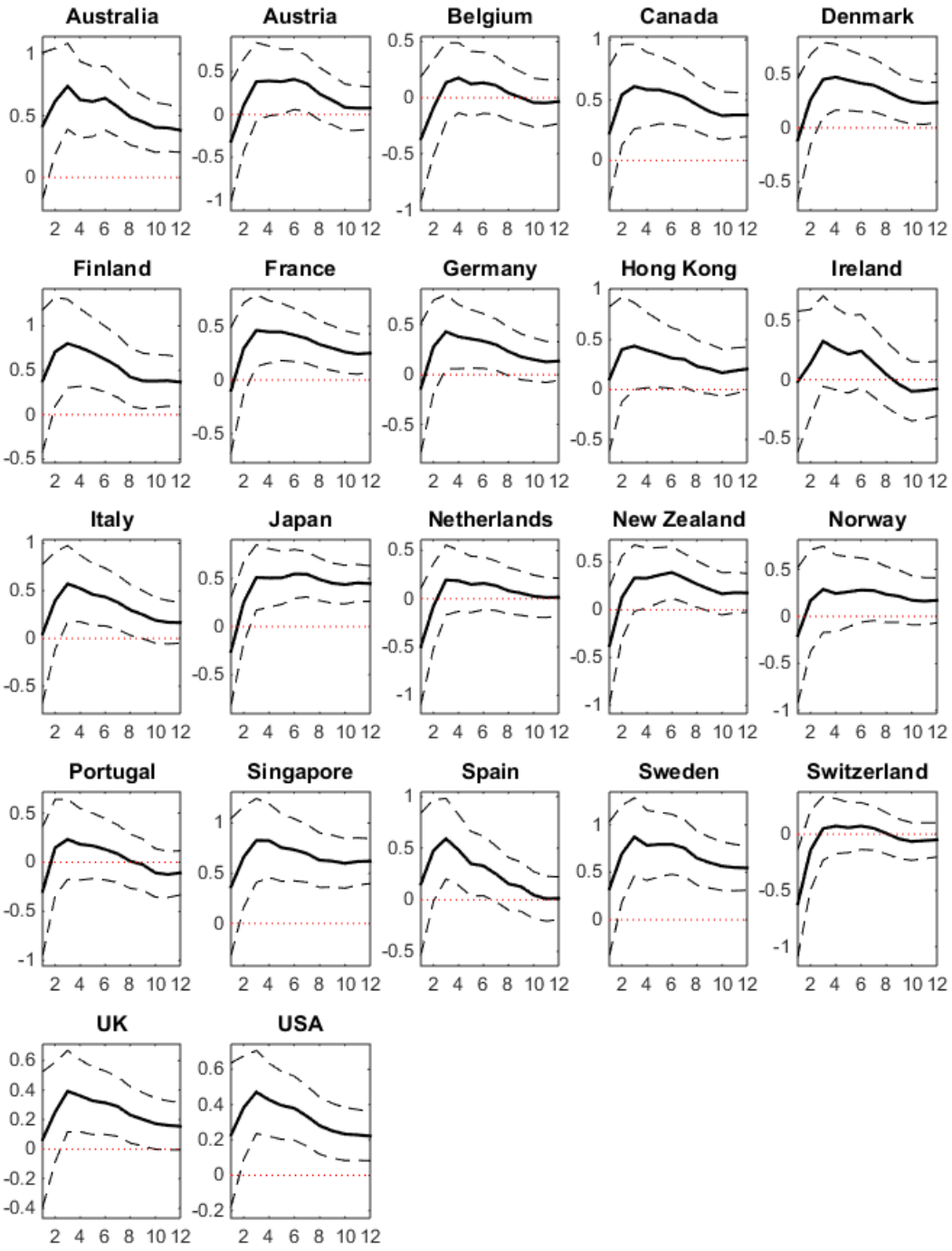

Figure 7: DVP predictive coefficients, Martingale measure

This figure shows the coefficient estimates of DVP from the country-level predictive regression specification (1), where DVP and UVP are the predictors. We use the Martingale measures of expected realized downside and upside variances to calculate alternative measures of the VP components (see Table 2). The dashed lines correspond to the 90% confidence intervals given NW standard errors.

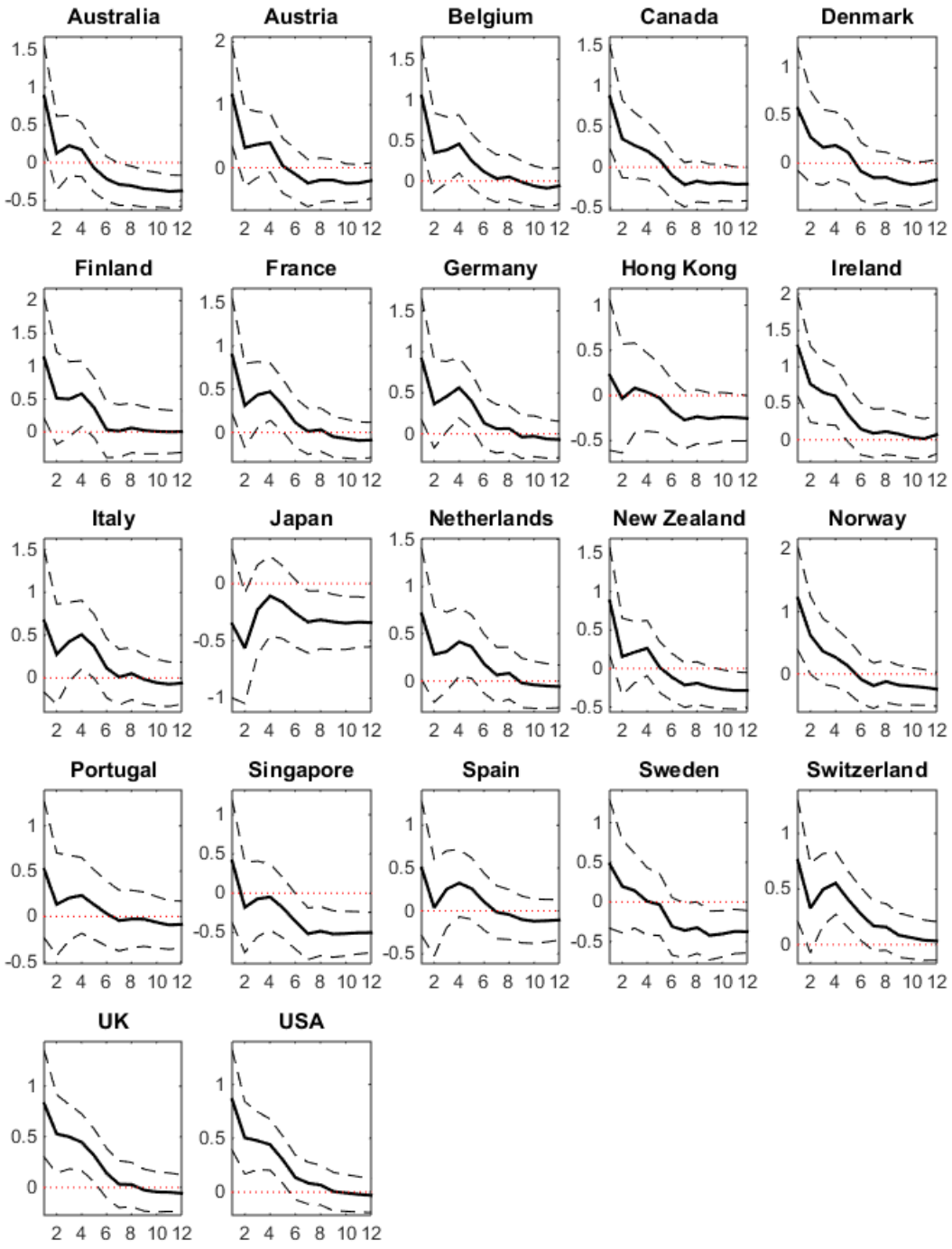

Figure 8: UVP predictive coefficients, Martingale measure

This figure shows the coefficient estimates of UVP from the country-level predictive regression specification (1), where DVP and UVP are the predictors. We use the Martingale measures of expected realized downside and upside variances to calculate alternative measures of the VP components (see Table 2). The dashed lines correspond to the 90% confidence intervals given NW standard errors.

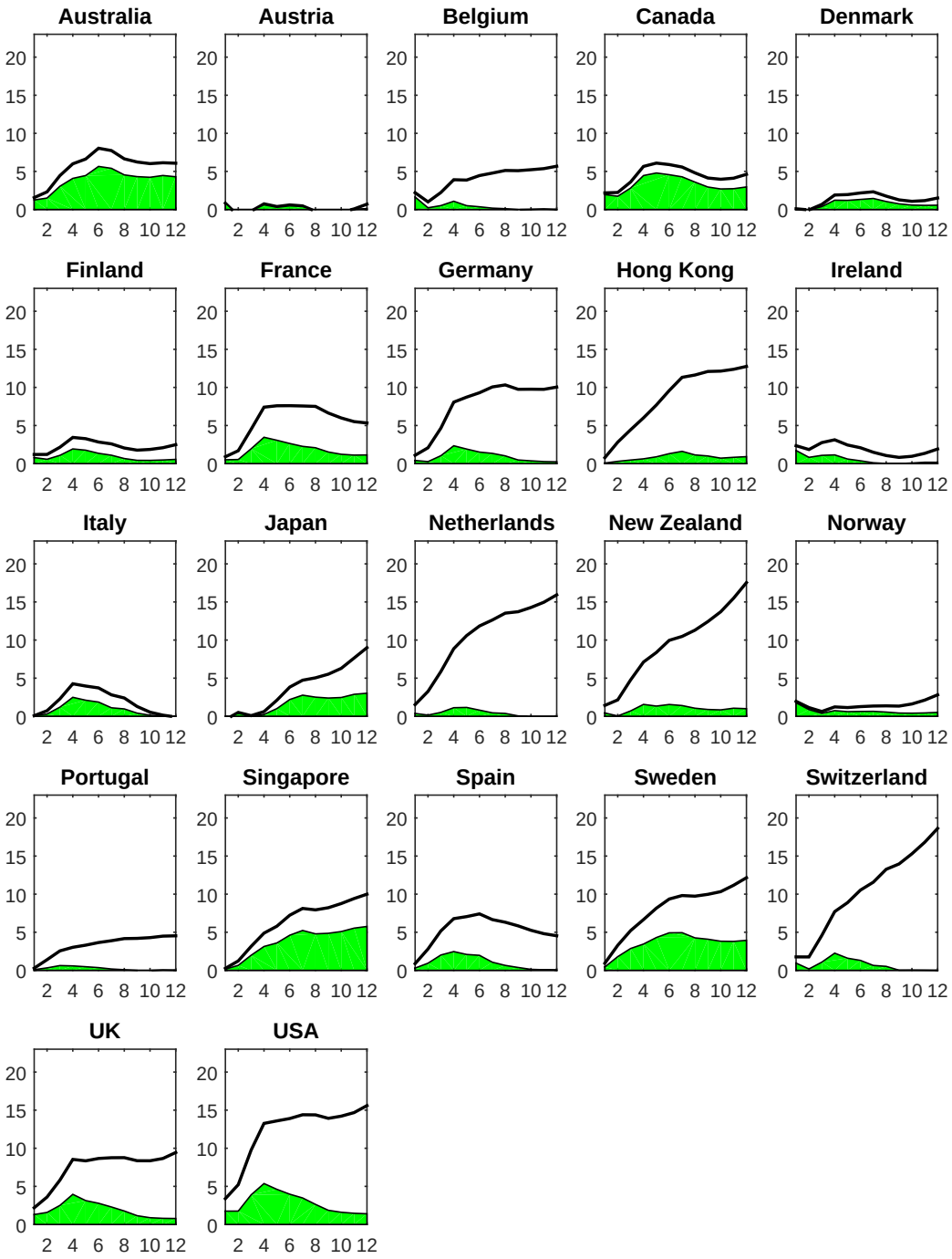

Figure 9: Explanatory power of DVP and UVP in the predictive model with control predictors

The solid line represents the total adjusted R^2 for the specification with DVP, UVP, the term spread, and the dividend yield as predictors (see Section 3). The green region represents the portion of R^2 that is explained by both upside and downside variance premiums.

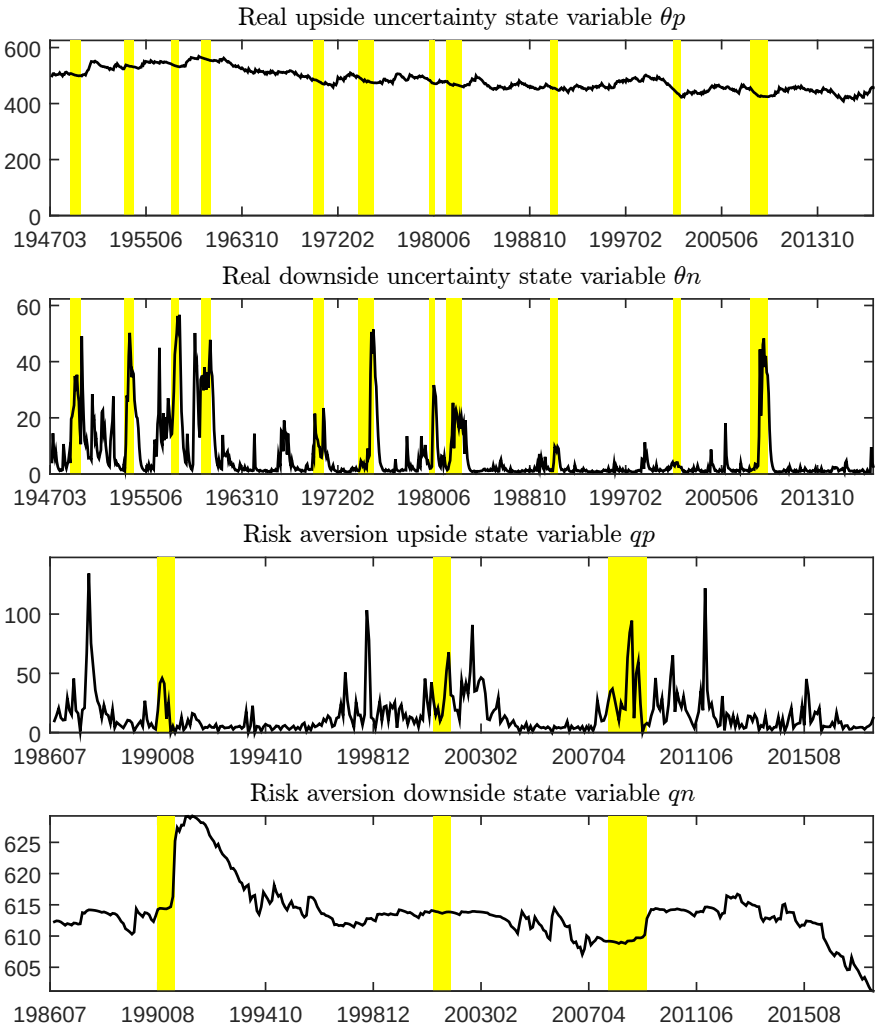

Figure 10: Global premium state variables

This figure shows the time series of empirical estimates of the four global premium state variables as derived in Section 4.3. From top to bottom: (1) real upside (θp) and (2) downside (θn) economic uncertainty state variables; and (3) risk aversion right-tail/upside (qp) and (4) left-tail/downside (qn) state variables. These four premium state variables are outputs from Tables B1 and B2 of the Appendix. Shaded regions indicate NBER recessions.

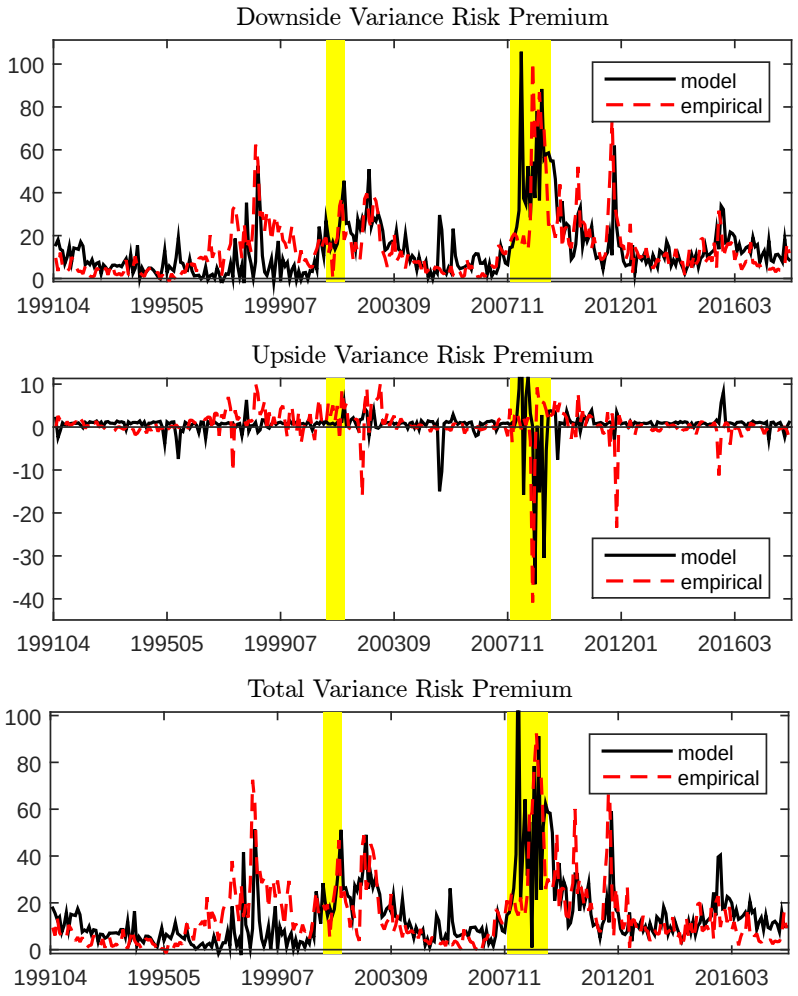

Figure 11: Model-implied and empirical variance risk premium components (first two plots) and total variance risk premium (bottom)

Shaded regions indicate NBER recessions.

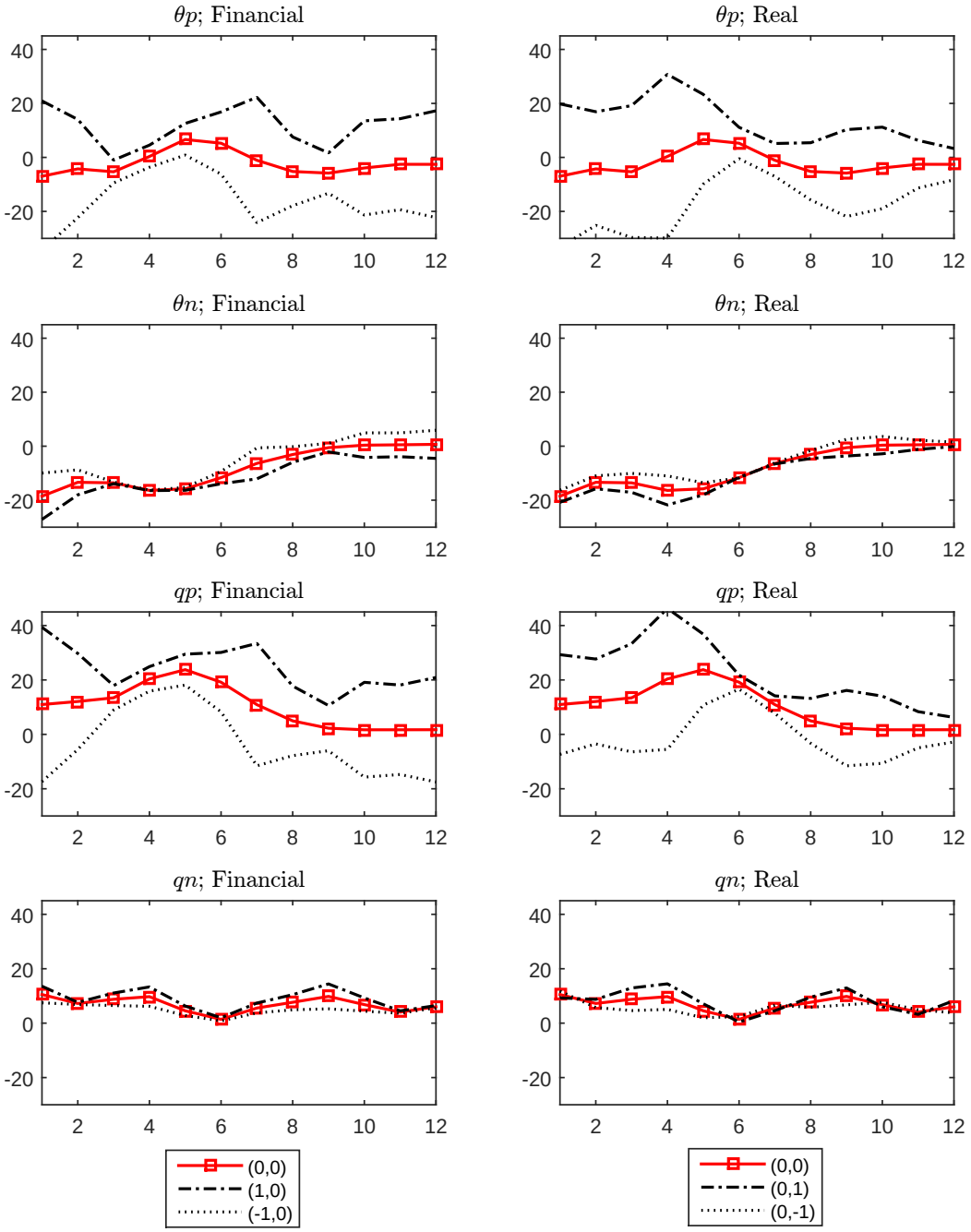

Figure 12: Relative economic magnitudes of equity risk premium loadings on premium state variables

This figure shows the effects of 1 standard deviation (SD) increase in the four global premium state variables on country equity premiums at different horizons, for countries with different integration characteristics. In particular, the red lines with squares depict the effects of 1 SD increase in a particular global state variable on the (annualized) equity risk premium for an average country (0,0); this line is the same for the two plots in the same row. The black dashed lines correspond to the effects of 1 SD increase in a particular global state variable on the (annualized) equity risk premium, however, for countries that are more integrated: trade-to-GDP ratio is +1 SD above average (left), and credit-to-GDP ratio is +1 SD above average (right). Similarly, the dotted black lines depict the less integrated countries. As an example, in the third row, the effect of the upside risk aversion state variable qp on country equity risk premiums is $[\widehat{v}_{qp,h,0} + \widehat{v}_{qp,h,2}E(z_t)] \times SD(qp_t)$ for an average country (red line with squares), $[\widehat{v}_{qp,h,0} + \widehat{v}_{qp,h,1,Trade} + \widehat{v}_{qp,h,2}E(z_t)] \times SD(qp_t)$ for a country with a higher/lower real integration (left panel), and $[\widehat{v}_{qp,h,0} + \widehat{v}_{qp,h,1,Credit} + \widehat{v}_{qp,h,2} * E(z_t)] \times SD(qp_t)$ for a country with a higher/lower financial integration (right panel).

Appendix

A. Solve price-dividend ratio and log stock returns (Section 4.3)

The price-dividend ratio can be rewritten as,

$$PD_t = E_t\left[M_{t+1}\left(\frac{P_{t+1}+D_{t+1}}{D_t}\right)\right] \sum_{n=1}^{\infty} E_t\left[\exp\left(\sum_{j=1}^{n} m_{t+j} + \Delta d_{t+j}\right)\right].$$

Let F_t^n denote the n-th term in the summation: $F_t^n = E_t\left[\exp\left(\sum_{j=1}^{n} m_{t+j} + \Delta d_{t+j}\right)\right]$, and $F_t^n D_t$ is the price of zero-coupon equity that matures in n periods. To show that equity price is an approximate affine function of the state variables, we first prove that $F_t^n (\forall n \geq 1)$ is exactly affine using induction. Rewrite the dividend growth process in a matrix representation, $\Delta d_{t+1} = d_0 + \boldsymbol{d_1 Y_t} + \boldsymbol{d_2 \Sigma \omega_{t+1}}$. First, when $n = 1$,

$$F_t^1 = E_t\left[\exp\left(m_{t+1} + \Delta d_{t+1}\right)\right] = E_t\left\{\exp\left[(m_0 + d_0) + \boldsymbol{(m_1 + d_1) Y_t} + \boldsymbol{(m_2 + d_2)\Sigma \omega_{t+1}}\right]\right\} = \exp\left(e_0^1 + \boldsymbol{e_1^1 Y_t}\right).$$

Now, suppose that the $(n-1)$-th term $F_t^{n-1} = \exp\left(e_0^{n-1} + \boldsymbol{e_1^{n-1} Y_t}\right)$, then

$$F_t^n = E_t\left[\exp\left(\sum_{j=1}^{n} m_{t+j} + \Delta d_{t+j}\right)\right] = E_t\left\{\exp(m_{t+1} + \Delta d_{t+1}) \underbrace{E_{t+1}\left[\exp\left(\sum_{j=1}^{n-1} m_{t+j+1} + \Delta d_{t+j+1}\right)\right]}_{F_{t+1}^{n-1}}\right\}$$

$$= E_t\left[\exp(m_{t+1} + \Delta d_{t+1}) \exp\left(e_0^{n-1} + \boldsymbol{e_1^{n-1} Y_{t+1}}\right)\right] = \exp\left(e_0^n + \boldsymbol{e_1^n Y_t}\right),$$

where e_0^n and $\boldsymbol{e_1^n}$ are defined implicitly. Hence, the price-dividend ratio can be solved as $PD_t = \sum_{n=1}^{\infty} F_t^n = \sum_{n=1}^{\infty} \exp\left(e_0^n + \boldsymbol{e_1^n Y_t}\right)$. Log return can be solved and approximated as,

$$\begin{aligned} r_{t+1} &= \ln\left(\frac{P_{t+1}+D_{t+1}}{P_t}\right) = \Delta d_{t+1} + \ln\left[\frac{1 + \sum_{n=1}^{\infty} \exp\left(e_0^n + \boldsymbol{e_1^n Y_{t+1}}\right)}{\sum_{n=1}^{\infty} \exp\left(e_0^n + \boldsymbol{e_1^n Y_t}\right)}\right] \\ &\approx \Delta d_{t+1} + \text{const.} + \frac{\sum_{n=1}^{\infty} \exp\left(e_0^n + \boldsymbol{e_1^n \bar{Y}}\right) \boldsymbol{e_1^n}}{\frac{1+\sum_{n=1}^{\infty} \exp\left(e_0^n + \boldsymbol{e_1^n \bar{Y}}\right)}{\sum_{n=1}^{\infty} \exp\left(e_0^n + \boldsymbol{e_1^n \bar{Y}}\right)}} \boldsymbol{Y_{t+1}} - \frac{\sum_{n=1}^{\infty} \exp\left(e_0^n + \boldsymbol{e_1^n \bar{Y}}\right) \boldsymbol{e_1^n}}{\sum_{n=1}^{\infty} \exp\left(e_0^n + \boldsymbol{e_1^n \bar{Y}}\right)} \boldsymbol{Y_t} \\ &= \xi_0 + \boldsymbol{\xi_1 Y_t} + \boldsymbol{\xi_2 \Sigma \omega_{t+1}}. \end{aligned}$$

The appendices of Xu (2019) and Bekaert, Engstrom, and Xu (2020) provide similar proofs of solving a no-arbitrage asset pricing model with gamma shocks. Both their and our derivation fully take advantage of the fact that the MGF of a gamma shock falls within an exponential affine class.

B. Additional Tables

Table B1: Estimation results of real upside and downside uncertainty state variables

This table reports the estimation results of real upside and downside economic uncertainty state variables (θp_t and θn_t, respectively). The log change in the monthly U.S. industrial production index is denoted by θ_t and is assumed with the following process:

$$\begin{aligned}\theta_{t+1} &= \theta_0 + \rho_{\theta\theta}\theta_t + \rho_{\theta\theta p}(\theta p_t - \overline{\theta p}) + \rho_{\theta\theta n}(\theta n_t - \overline{\theta n}) + u_{\theta,t+1},\\ u_{\theta,t+1} &= \delta_{\theta\theta p}\omega_{\theta p,t+1} - \delta_{\theta\theta n}\omega_{\theta n,t+1},\end{aligned}$$

where

$$\begin{aligned}\omega_{\theta p,t+1} &\sim \Gamma(\theta p_t, 1) - \theta p_t,\\ \omega_{\theta n,t+1} &\sim \Gamma(\theta n_t, 1) - \theta n_t,\\ \theta p_{t+1} &= \overline{\theta p} + \rho_{\theta p}(\theta p_t - \overline{\theta p}) + \delta_{\theta p}\omega_{\theta p,t+1},\\ \theta n_{t+1} &= \overline{\theta n} + \rho_{\theta n}(\theta n_t - \overline{\theta n}) + \delta_{\theta n}\omega_{\theta n,t+1}.\end{aligned}$$

We follow Bekaert, Engstrom, and Xu (2020) and set the mean of θp_t to be 500. In their paper, they survey and estimate a wide range of models and find that imposing a constant in the mean of θp_t improves the BIC criteria without loosing the model efficiency. The estimation is conducted using the Approximate Maximum Likelihood (AML) methodology in Bates (2006). Other model details are described in Section 4. *** (**, *) represent significance at the 1% (5%, 10%) confidence level. Panel B shows moment matching. In this panel, values under "Model" are in bold if the model-implied moments are within the 95% confidence interval of data point estimates. Panel C provides a cyclicality test and shows the correlations between uncertainty state variables and the NBER recession indicator.

A. Estimation Results					
	θ_t		θp_t		θn_t
θ_0	0.0015***	$\overline{\theta p}$	500 (fix)	$\overline{\theta n}$	10.3362***
	(0.0003)				(2.0747)
$\rho_{\theta\theta}$	0.3818***	$\rho_{\theta p}$	0.9979***	$\rho_{\theta n}$	0.9525***
	(0.0316)		(0.0171)		(0.0096)
$\rho_{\theta\theta p}$	0.0000				
	(0.0002)				
$\rho_{\theta\theta n}$	-0.0001				
	(0.0012)				
$\delta_{\theta\theta p}$	0.0001***	$\delta_{\theta p}$	0.3739***		
	(0.0000)		(0.0173)		
$\delta_{\theta\theta n}$	0.0028***			$\delta_{\theta p}$	2.2996***
	(0.0003)				(0.1907)

B. Moment Match			C. Cyclicality		
	Data	Model		θp_t	θn_t
Mean	0.0022***	**0.0024**	$\rho(NBER)$	-0.0201	0.6012***
	(0.0003)			(0.0512)	(0.0409)
Variance	5.8E-5***	**6.7E-5**			
	(7.7E-6)				

Table B2: Estimation results of upside and downside risk aversion state variables

This table reports the estimation results of upside (right-tail) and downside (left-tail) state variables of risk aversion (qp_t and qn_t, respectively). These two state variables capture the tail variability of risk aversion, and are extracted from a monthly risk aversion index constructed by Bekaert, Engstrom, and Xu (2020). The risk aversion state variable is denoted by q_t and is assumed with the following process:

$$q_{t+1} = q_0 + \rho_{qq} q_t + \rho_{q\theta p}(\theta p_t - \overline{\theta p}) + \rho_{q\theta n}(\theta n_t - \overline{\theta n}) + \rho_{qqp}(qp_t - \overline{qp}) + \rho_{qqn}(qn_t - \overline{qn}) + u_{q,t+1},$$
$$u_{q,t+1} = \delta_{q\theta p}\omega_{\theta p,t+1} + \delta_{q\theta n}\omega_{\theta n,t+1} + \delta_{qqp}\omega_{qp,t+1} - \delta_{qqn}\omega_{qn,t+1},$$

where

$$\omega_{qp,t+1} \sim \Gamma(qp_t, 1) - qp_t,$$
$$\omega_{qn,t+1} \sim \Gamma(qn_t, 1) - qn_t,$$
$$qp_{t+1} = \overline{qp} + \rho_{qp}(qp_t - \overline{qp}) + \delta_{qp}\omega_{qp,t+1},$$
$$qn_{t+1} = \overline{qn} + \rho_{qn}(qn_t - \overline{qn}) + \delta_{qn}\omega_{qn,t+1}.$$

The estimation is conducted in two stages; (1), we project q_{t+1} onto $\{q_t, \theta p_t, \theta n_t, \omega_{\theta p,t+1}, \omega_{\theta n,t+1}\}$ where $\theta p_t, \theta n_t, \omega_{\theta p,t+1}, \omega_{\theta n,t+1}$ are estimated from Table B1; (2), we estimate latent processes using AML in Bates (2006). Other model details are described in Section 4. *** (**, *) represent significance at the 1% (5%, 10%) confidence level. Panel B shows moment matching. In this panel, values under "Model" are in bold if the model-implied moments are within the 95% confidence interval of data point estimates. Panel C provides a cyclicality test and shows the correlations between risk aversion state variables and the NBER recession indicator.

A. Estimation Results					
	q_t		qp_t		qn_t
q_0	0.1298***	$\overline{qp}$	14.5891***	$\overline{qn}$	612.3177***
	(0.0239)		(0.9812)		(44.1574)
ρ_{qq}	0.7142***	ρ_{qp}	0.6352***	ρ_{qn}	0.9999***
	(0.0367)		(0.0229)		(0.0315)
$\rho_{q\theta p}$	0.0003				
	(0.0003)				
$\rho_{q\theta n}$	0.0036***				
	(0.0010)				
ρ_{qqp}	0.0000				
	(0.0016)				
ρ_{qqn}	-0.0001*				
	(0.0001)				
$\delta_{q\theta p}$	0.0007*	δ_{qp}	3.291***		
	(0.0004)		(0.2166)		
$\delta_{q\theta n}$	0.0195***			δ_{qp}	0.0044
	(0.0039)				(0.0140)
δ_{qqp}	0.0209***				
	(0.0041)				
δ_{qqn}	0.0008				
	(0.0011)				

B. Moment Match			C. Cyclicality		
	Data	Model		qp_t	qn_t
Mean	0.3068***	**0.3102**	$\rho(NBER)$	0.2546***	-0.1118**
	(0.0084)			(0.0495)	(0.0508)
Variance	0.0084*	**0.0094**			
	(0.0045)				